Design and Synthesis of Potential Pyrrole Coupled Carbothioamide Derivatives and its Antibacterial Studies against Superbug MRSA

BoobalArasu Velu [1],* , GanesamoorthyThirunarayanan [1],* , Sivakumar Kulanthaivel [2]

1   Department of Chemistry, Annamalai University, Annamalai nagar-608002, Tamil Nadu, India
2   Department of Chemistry, Adhiyamaan College of Engineering, Hosur-635109, Tamil Nadu, India
*   Correspondence: boobalarasuvelu73@gmail.com (B.A.V); drgtnarayanan@gmail.com (G.T);

Abstract: MRSA (Methicillin-resistant *Staphylococcus aureus*) is a contagious bacterial infection resistant to numerous antibiotics. This resistance makes treatment difficult. The infection rate of MRSA has tremendously increased globally, and it is very hard to eradicate clinically associated infections. To tackle MRSA infections, a new antibacterial contender, pyrrole coupled carbothioamide derivatives, has been synthesized and amply characterized by various studies, viz UV-Visible spectra, FTIR, ^{1}H-NMR, ^{13}C-NMR, and LCMS. All the derivatives have been assessed for their ADME, bioactive score, pharmacophore model, PASS, and BBB. All the derivatives were assessed for antibacterial activity;5d had shown potent antibacterial activity against MRSA. It was found to be 18±0.20 µg/mL and 17.10±0.05 ZOI in mm compared to streptomycin (10 µg/mL) and vancomycin (30 µg/disc), respectively. The antibacterial property was recognized by a membrane damage study of MRSA by SEM images, cellular content leakage, potassium efflux, and bacterial respiration inhibition and also validated by an *in-silico* molecular docking study against MRSA protein 6FTB. The docking study showed a good binding score of -6.95 compared to Streptomycin (-7.56). 5d had also inactivated the MRSA coagulase at 25µg/mL by blocking the conversion of soluble fibrinogen to insoluble fibrin clots in rabbit plasma compared to Dabigatran (10µg/mL). 5d was more biocompatible, evident from the less damage it caused to RBC cells (up to 1000 µg/mL). The toxicity of 5d was tested against 3T3-L1 cell lines, it showed an IC_{50} value of 357.50 µg/mL, and that of Doxorubicin was 28.21µg/mL. This revealed that 5d analog could be a warranted drug candidate to tackle MRSA infections.

Keywords: pyrrole-coupled carbothioamide; antibacterial activity; molecular docking; biocompatibility; toxicity.

1. Introduction

Pyrrole has the chemical formula C_4H_5N and is an aromatic five-membered ring. In 1834, F.F. Runge discovered it as a component of coal tar. Further investigation revealed that it was isolated from bone pyrolusite in 1857. Fischer produced haemin, one of the first pyrrole-containing molecules, in 1929. It is a colorless volatile liquid that darkens quickly when exposed to air and polymerizes when exposed to light. Pyrroles are less basic than amines and other aromatic compounds with pyridine as a component [1]. Pyrrole is a classic heteroaromatic molecule, and as such, both experiment and theory have focused on understanding its electronic structure and photochemistry [2].

Pyrroles are significant molecules that can be found in a wide range of natural goods, pharmaceuticals, catalysts, and materials. The pyrrole porphobilinogen is used to biosynthesize the blood respiratory pigment haem and the green photosynthetic pigment chlorophyll. The bioactive component of the best-selling medicine by value is a pyrrole derivative. Polypyrroles are conductive polymers that are utilized in solar cells and batteries. Pyrrole can be synthesized using a variety of traditional procedures and catalytic reactions. The recent flurry of catalytic procedures published demonstrates the burgeoning interest in this subject. Because of the great demand for innovative reactions that use renewable resources as well as the importance of pyrroles, a pyrrole synthesis that employs renewable resources entirely or partially is a highly desirable goal. In pharmacology, material sciences, and natural goods, indoles and pyrroles have a unique place. Heterocyclic can be used as additives and modifiers in various industries, including cosmetics, polymers, solvents, and antioxidants. As a result, one of the key goals of modern researchers is to synthesize heterocyclic molecules. Pyrrole has attracted a lot of attention among novel heterocyclic compounds because of its biological potential as an antimalarial and enzyme inhibitor. Pyrrole derivatives can be discovered as co-factors and natural products in a variety of biological contexts. Vitamin B12, bile pigments including bilirubin and biliverdin, hemi-porphyrins, chlorophyll, chlorins, bacteriochlorins, and porphyrinogens are all examples of naturally occurring pyrrole-containing compounds. Pyrrole derivatives are physiologically active heterocyclic compounds that can be used as scaffolds for antibacterial, anti-viral, antimalarial, antitubercular, anti-inflammatory, and enzyme inhibitor medicines.

Researchers are encouraged to develop novel pyrrole derivatives for treating multi-drug resistant (MDR) infections because of their unrivaled anticancer and antitubercular characteristics [3-5]. Pyrrole has gotten a lot of attention among the newer heterocyclic moieties because of its pharmacological effects. Its increasing abundance in natural goods, medicines, and new materials has pushed pyrrole and its derivatives chemically into the spotlight. The delocalization of the nitrogen lone pair of electrons in the pyrrole ring causes the drop in basicity. Pyrrole has a pKa of 3.8, and protonation causes pyrrole to lose its aromaticity. The pyrrole moieties –NH– and –CH– protons are moderately acidic and can be deprotonated with strong bases, making the pyrrole ring a nucleophile by nature. Antihypertensive drugs, antimalarial drugs, antiulcer drugs, mGluR1 antagonists, DPP IV inhibitors, insecticides, histone deacetylase inhibitors, cannabinoid receptor antagonists, allosteric modulators of AMPA, dopaminergic receptor antagonists, progesterone receptor antagonists, GnRH antagonists, androgen antagonists, neuroprotective GSNOR inhibitors, and dual orexin receptor antagonists Furthermore, they are found in polymers and bigger aromatic rings.

Superbug MRSA is one of the important causes of HAinfections (hospital-acquired) and CA-infections (community-associated) and is usually associated with large morbidity and mortality. Multi-Drug Methicillin-resistant *Staphylococcus aureus* (MD-MRSA) is one of the most perilous human pathogens and a generally evolving zoonotic pathogen with implications for public health. In humans, MRSA recurrently causes severe infectious diseases, including food poisoning, pyogenic endocarditis, suppurative pneumonia, otitis media, osteomyelitis, and pyogenic infections of the skin and soft tissues. The regular usage of antibiotics in humans and animals is causing the development of MDR-MRSA. The health tactic of MDR-MRSA infections needs the association between public health experts, epidemiologists, microbiologists, and medical clinicians. Today, MRSA infections are more resistant to viable antibiotics [6]. To address the growing problem of antibiotic resistance in animals and humans,

we must investigate, design, and synthesize new potential organic derivatives. This study aimed to design and synthesize pyrrole-coupled carbothioamide derivatives to tackle MD-MRSA infections. *In vitro* and molecular docking studies were conducted to assess the potency of the antibacterial activity of derivatives.

2. Materials and Methods

2.1. Chemicals.

All chemicals and reagents were purchased from Sigma Aldrich and Merck Chemical Pvt-Ltd and were not purified further. Using an Agilent Cary 630 FT-IR spectrometer, the IR spectra were obtained. At room temperature, all of the spectra were performed in the 400-4000 cm^{-1} range. NMR spectra in CDCl$_3$ were obtained at 400MHz, and all chemical shifts were recorded in ppm relative to TMS. In a Water micro TOF QII mass spectrometer, mass spectroscopic analysis was done.

2.2. Synthesis of pyrrole derivatives (5a-1).

2.2.1 Synthesis of (N-(2-piperazin-1-yl) ethyl)-1-(1H-pyrrol-2-yl) methenamine (3).

Equimolar concentrations of Pyrrole-2-carboxaldehyde (0.5gm, 1 equi) 1-(2-aminoethyl) piperazine (2equi) were refluxed for 4-5 hrs in methanol (25 mL) and then 2-3 drops of acetic acid were added to the mixture. The reaction completion was confirmed by thin-layer chromatography (TLC). The solvent was concentrated, and the solid was dried and recrystallized from methanol. The brownish product (3) was obtained with a good yield (Figure 1).
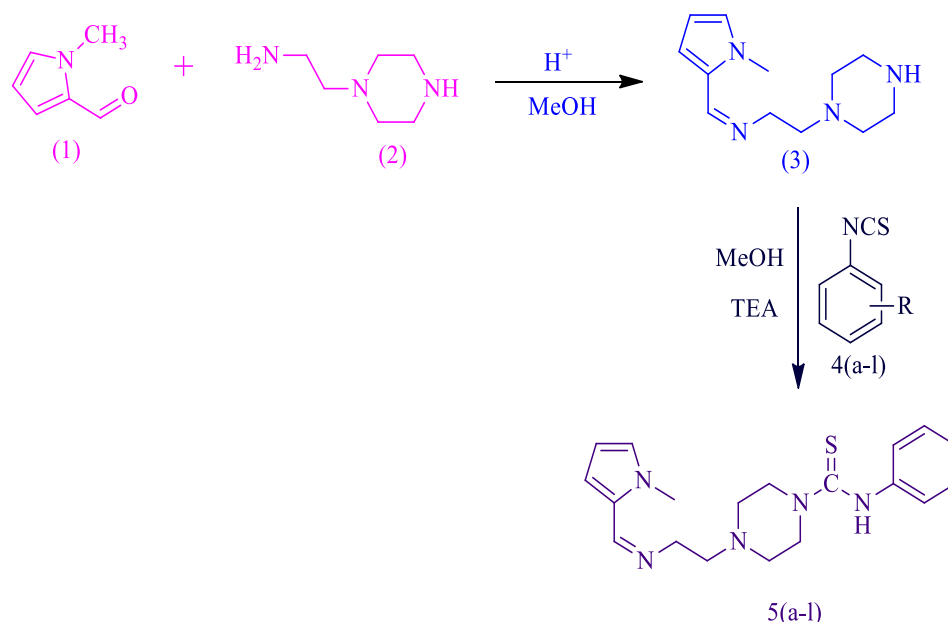
Figure 1. Scheme for synthesis of 5(a-1) compounds.

2.2.2. Synthesis of (Z)-4-(2-(((1-methyl-1H-pyrrol-2-yl)methylene)amino)ethyl)-N-phenylpiperazine-1-carbothioamide (5a-1).

A solution of (N-(2-piperazin-1-yl) ethyl)-1-(1H-pyrrol-2-yl) methanimine and 1-isothiocyanato -4 -methylbenzene was refluxed for 4-5 hrs in methanol (25 mL) and then 2-3 drops of triethylamine were added to the mixture. The reaction completion was confirmed by

thin-layer chromatography (TLC). The solvent was concentrated, and the solid was dried and recrystallized from methanol. The product was obtained in good yield (Figure 1). The synthesized compound's structure is tabulated in table 1.

2.2.2.1. (Z)-4-(2-(((1H-pyrrol-2-yl) methylene) amino) ethyl)-N-phenylpiperazine-1-carbothioamide (5a).

Obtained 85% yield, column chromatography: used petroleum ether/ethyl acetate (2:3) v/v as solvent. ^{1}H NMR (CDCl$_3$,400 MHz), 7.31 (d, 2H, Ar-H) 7.43 (t, 2H, Ar-H) 7.09 (t, 1H, Ar-H) 9.26 (s, 1H, N-H) 3.68 (t, 4H, Pip-H) 2.46 (t, 4H, Pip-H) 2.4 (t, 2H, CH$_2$) 1.61 (t, 2H, CH$_2$) 8.28(s, 1H, C=N) 6.79 (d, 1H, Pyr-H) 6.22(t,1H, Pyr-H) 7.15 (d, 1H, Pyr-H) 3.91 (s, 3H, CH$_3$) ^{13}C NMR: (400Hz, CDCl$_3$) 128.4 (Ar-C) 129.0 (Ar-C) 126.5 (Ar-C) 138.5 (Ar-C) 57.1 (Pip-C) 56.7 (Pip-C) 62.1(CH$_2$) 47.1 (CH$_2$) 132.3 (Pyr-C) 122.7 (Pyr-C) 108.7 (Pyr-C) 129.0 (Pyr-C) 38.1 (CH$_3$) 153.7 (imine-C) 181.8 (sulfide-C) LCMS m/z Calculated for C$_{19}$H$_{25}$N$_5$S: 355.18 IR Vmax (cm-1) 3360 (N-H), 1670 (C=C), 1320 (C-N), 1690 (C=N) Elemental Analysis: Calculated: C,64.19; H,7.09; N, 19.70; S, 9.02; Experimental: C, 64.18; H,7.06; N, 19.69;S,9.01.

2.2.2.2. (Z)-4-(2-(((1H-pyrrol-2-yl)methylene)amino)ethyl)-N-(p-tolyl) piperazine carbothioamide (5b).

In column chromatography: solvent system petroleum ether/ethyl acetate (2:3) v/v was used and obtained 83% yield.^{1}H NMR (CDCl$_3$,400 MHz). 7.37 (d, 4H, Ar-H) 2.32 (s, 3H,CH$_3$) 9.26 (s, 1H, N-H) 3.68 (t, 4H, Pip-H) 2.46 (t, 4H, Pip-H) 2.4 (t, 2H, CH2) 1.61 (t, 2H, CH$_2$) 8.28(s, 1H, C=N) 6.79 (d, 1H, Pyr-H) 6.22 (t,1H, Pyr-H) 7.15 (d, 1H, Pyr-H) 3.91 (s, 3H, CH$_3$) ^{13}C NMR: (400Hz, CDCl$_3$) 129.3 (Ar-C) 126.4 (Ar-C) 137.2 (Ar-C) 135.5 (Ar-C) 21.3 (CH$_3$) 57.1 (Pip-C) 56.7 (Pip-C) 62.1(CH$_2$) 47.1 (CH$_2$) 132.3 (Pyr-C) 122.7 (Pyr-C) 108.7 (Pyr-C) 129.0 (Pyr-C) 38.1(CH$_3$) 153.7 (imine-C) 181.8 (sulfide-C) LCMS m/z Calculated for C$_{20}$H$_{27}$N$_5$S: 369.20 IR Vmax (cm-1) 3360 (N-H), 1670 (C=C), 1320 (C-N), 1690 (C=N) Elemental Analysis: Calculated: C,68.44; H, 7.66; N, 15.20; S, 8.70 Experimental: C,68.41;H, 7.65; N, 15.16; S, 8.68.

2.2.2.3. (Z)-4-(2-(((1H-pyrrol-2-yl) methylene) amino) ethyl)-N-(4-methoxyphenyl) piperazine-1-carbothioamide(5c).

In column chromatography: the solvent system petroleum ether/ethyl acetate (2:3) v/v was used and obtained 87% yield. ^{1}H NMR (CDCl$_3$,400 MHz). 7.44 (d, 2H, Ar-H) 6.90 (d, 2H,C=S) 9.26 (s, 1H, N-H) 3.68 (t, 4H, Pip-H) 2.46 (t, 4H, Pip-H) 2.4 (t, 2H, CH2) 1.61 (t, 2H, CH$_2$) 8.28(s, 1H, C=N) 7.15 (d, 1H, Pyr-H) 6.22 (t,1H, Pyr-H) 6.79 (d, 1H, Pyr-H) 3.91(s,3H, CH$_3$) 3.81(s,3H,OCH$_3$) ^{13}C NMR: (400Hz, CDCl$_3$) 114.6 (Ar-C) 127.5 (Ar-C) 113.3 (Ar-C) 159.3 (Ar-C) 55.8 (O-CH3) 57.1 (Pip-C) 56.7 (Pip-C) 62.1(CH$_2$) 47.1 (CH$_2$) 132.3 (Pyr-C) 122.7 (Pyr-C) 108.7 (Pyr-C) 129.0(Pyr-C) 38.1(CH$_3$) 153.7 (imine-C) 181.8 (sulfide-C) LCMS m/z Calculated for C$_{20}$H$_{27}$N$_5$OS; 385.19 IR Vmax (cm-1) 3360 (N-H), 1670 (C=C), 1320 (C-N), 1690 (C=N) Elemental Analysis: Calculated: C,61.43; H,6.78; N, 18.85; S,8.63; O,4.31;Experimental:C,61.42; H,6.76; N, 18.82; S,8.62; O,4.30.

2.2.2.4. (Z)-4-(2-(((1H-pyrrol-2-yl) methylene) amino) ethyl)-N-(4-hydroxyphenyl) piperazine-1-carbothioamide(5d).

In column chromatography: solvent system petroleum ether/ethyl acetate (2:3) v/v was used and obtained 88% yield.^{1}H NMR (CDCl$_3$,400 MHz). 7.27 (d, 2H, Ar-H) 6.70 (d, 2H,Ar-H) 9.26 (s, 1H, N-H) 9.44 (s, 1H, O-H) 3.68 (t, 4H, Pip-H) 2.46 (t, 4H, Pip-H) 2.4 (t, 2H, CH$_2$) 1.61 (t, 2H, CH$_2$) 8.28(s, 1H, C=N) 6.79 (d, 1H, Pyr-H) 6.22 (t,1H, Pyr-H) 7.15 (d, 1H, Pyr-H) 3.91 (s,3H,CH$_3$) ^{13}C NMR: (400Hz, CDCl$_3$) 116.2 (Ar-C) 127.9 (Ar-C) 154.5 (Ar-C) 113.6 (Ar-C) 57.1 (Pip-C) 56.7 (Pip-C) 62.1(CH$_2$) 47.1 (CH$_2$) 132.3 (Pyr-C) 122.7 (Pyr-C) 108.7 (Pyr-C) 129 (Pyr-C) 38.1(CH$_3$) 153.7 (imine-C) 181.8 (sulfone-C) LCMS m/z Calculated for C$_{19}$H$_{25}$N$_5$OS: 371.18 IR Vmax (cm-1) 3360 (N-H), 1670 (C=C), 1320 (C-N), 1690 (C=N) Elemental Analysis: Calculated: C,61.43; H,6.78; N,18.85; S,8.63 ; O,4.31; Experimental:C,61.42; H,6.75; N, 18.84;S,8.61; O,4.30;.

2.2.2.5. (Z)-4-(2-(((1H-pyrrol-2-yl) methylene) amino) ethyl)-N-(4-chlorophenyl) piperazine-1-carbothioamide (5e).

In column chromatography: solvent system petroleum ether/ethyl acetate (2:3) v/v was used and obtained 92% yield.^{1}H NMR (CDCl$_3$, 400 MHz). 7.37 (d, 2H, Ar-H) 7.61 (d, 2H,Ar-H) 9.26 (s, 1H, N-H) 3.68 (t, 4H, Pip-H) 2.46 (t, 4H, Pip-H) 2.4 (t, 2H, CH$_2$) 1.61 (t, 2H, CH$_2$) 8.28(s, 1H, C=N) 6.79 (d, 1H, Pyr-H) 6.22 (t,1H, Pyr-H) 7.15 (d, 1H, Pyr-H) 3.91(s,3H, CH$_3$) ^{13}C NMR: (400Hz, CDCl$_3$) 133.7(Ar-C) 129.1 (Ar-C) 131.1 (Ar-C) 136.6 (Ar-C) 57.1 (Pip-C) 56.7 (Pip-C) 62.1(CH$_2$) 47.1 (CH$_2$) 132.3 (Pyr-C) 122.7 (Pyr-C) 108.7 (Pyr-C) 129.0 (Pyr-C) 38.1(CH3) 153.7 (imine-C) 181.8 (sulfone-C) LCMS m/z Calculated for C$_{19}$H$_{24}$ClN$_5$S: 389.14 IR Vmax (cm-1) 3360 (N-H), (1670 (C=C), 1320 (C-N), 1690 (C=N) Elemental Analysis: Calculated: C, 58.52; H, 6.20; Cl, 9.09; N, 17.96; S, 8.22.Experimental C, 58.51; H, 6.18; Cl, 9.06; N, 17.94; S, 8.21.

2.2.2.6. (Z)-4-(2-(((1H-pyrrol-2-yl) methylene) amino) ethyl)-N-(3-chlorophenyl) piperazine-1-carbothioamide(5f).

In column chromatography: solvent system petroleum ether/ethyl acetate (2:3) v/v was used and obtained 79% yield.^{1}H NMR (CDCl$_3$, 400 MHz). 7.36 (t, 1H, Ar-H) 7.35 (d, 1H, Ar-H) 7.18 (d,1H, Ar-H) 7.79 (s,1H, Ar-H) 9.26 (s, 1H, N-H) 3.68 (t, 4H, Pip-H) 2.46 (t, 4H, Pip-H) 2.4 (t, 2H, CH$_2$) 1.61 (t, 2H, CH$_2$) 8.35(s, 1H, C=N) 6.51 (d, 1H, Pyr-H) 6.15 (t,1H, Pyr-H) 6.95 (d, 1H, Pyr-H) 3.91(s,3H, CH$_3$) ^{13}C NMR: (400Hz, CDCl$_3$) 138.5(Ar-C) 124.6 (Ar-C) 130.4 (Ar-C) 128.3 (Ar-C) 134.6(Ar-C)126.9 (Ar-C) 57.1 (Pip-C) 56.7 (Pip-C) 62.1(CH$_2$) 47.1 (CH$_2$) 132.7 (Pyr-C) 124.8 (Pyr-C) 119.2 (Pyr-C) 110.9 (Pyr-C) 38.1(CH$_3$) 153.7 (imine-C) 181.8 (sulfone-C) LCMS m/z Calculated for C$_{19}$H$_{24}$ClN$_5$S;389.14 IR V$_{max}$ (cm-1) 3360 (N-H), 1670 (C=C), 1320 (C-N), 1690 (C=N) Elemental Analysis calculated: C, 58.52; H, 6.20; Cl, 9.09; N, 17.96; S, 8.22.Experimental C, 58.51; H, 6.17; Cl, 9.08; N, 17.94; S, 8.18.

2.2.2.7. (Z)-4-(2-(((1H-pyrrol-2-yl) methylene) amino) ethyl)-N-(2-chlorophenyl) piperazine-1-carbothioamide(5g)

In column chromatography: solvent system petroleum ether/ethyl acetate (2:3) v/v was used and obtained 90% yield.^{1}H NMR (CDCl$_3$,400 MHz). 7.26 (t, 1H, Ar-H) 7.54 (d, 1H,Ar-H) 7.93 (d,1H, Ar-H) 7.38 (t,1H, Ar-H) 10.78 (s, 1H, N-H) 3.68 (t, 4H, Pip-H) 2.46 (t, 4H, Pip-H) 2.4 (t, 2H, CH$_2$) 1.61 (t, 2H, CH$_2$) 8.35(s, 1H, C=N) 6.51 (d, 1H, Pyr-H) 6.15 (t,1H,

Pyr-H) 6.95 (d, 1H, Pyr-H) 3.91(s,3H, CH$_3$) ^{13}C NMR: (400Hz, CDCl$_3$) 135.9(Ar-C) 133.9 (Ar-C) 124.3 (Ar-C) 131.4 (Ar-C) 130.2(Ar-C) 57.1 (Pip-C) 56.7 (Pip-C) 62.1(CH$_2$) 47.1 (CH$_2$) 132.7 (Pyr-C) 124.8 (Pyr-C) 119.2 (Pyr-C) 110.9 38.1(CH$_3$) (Pyr-C) 153.7 (imine-C) 181.8 (sulfone-C) LCMS m/z Calculated forC$_{19}$H$_{24}$ClN$_5$S: 389.14. IR V$_{max}$ (cm^{-1}) 3360 (N-H), 1670 (C=C), 1320 (C-N), 1690 (C=N) Elemental Analysis: CalculatedC, 58.52; H, 6.20; Cl, 9.09; N, 17.96; S, 8.22; Experimental; C, 58.51; H, 6.18; Cl, 9.07; N, 17.95; S, 8.20.

2.2.2.8. (Z)-4-(2-(((1H-pyrrol-2-yl) methylene) amino) ethyl)-N-(3,5-dichlorophenyl) piperazine-1-carbothioamide(5h).

In column chromatography: solvent system petroleum ether/ethyl acetate (2:3) v/v was used and obtained 85% yield.^{1}H NMR (CDCl^3,400 MHz). 7.47 (s, 1H, Ar-H) 7.67 (s, 2H,Ar-H) 9.26 (s, 1H, N-H) 3.68 (t, 4H, Pip-H) 2.46 (t, 4H, Pip-H) 2.4 (t, 2H, CH2) 1.61 (t, 2H, CH2) 8.35(s, 1H, C=N) 6.51 (d, 1H, Pyr-H) 6.15 (t,1H, Pyr-H) 6.95 (d, 1H, Pyr-H) 3.91(s,3H,CH$_3$) ^{13}C NMR: (400Hz, CDCl$_3$) 125.2(Ar-C) 129.3 (Ar-C) 125.0 (Ar-C) 139.9 (Ar-C) 57.1 (Pip-C) 56.7 (Pip-C) 62.1(CH2) 47.1 (CH2) 132.7 (Pyr-C) 124.8 (Pyr-C) 119.2 (Pyr-C) 110.9 (Pyr-C) 38.1(CH$_3$) 153.7 (imine-C) 181.8 (sulfone-C) LCMS m/z Calculated for C$_{19}$H$_{23}$Cl$_2$N$_5$S;423.11, IR V$_{max}$ (cm-1) 3360 (N-H), 1670 (C=C), 1320 (C-N), 1690 (C=N) Elemental Analysis: Calculated: C, 53.77; H, 5.46; Cl, 16.71; N, 16.50; S, 7.55,Experimental; C, 53.75; H, 5.42; Cl, 16.69; N, 16.48; S, 7.53.

2.2.2.9. (Z)-4-(2-(((1H-pyrrol-2-yl) methylene) amino) ethyl)-N-(4-fluorophenyl) piperazine-1-carbothioamide(5i).

In column chromatography: solvent system petroleum ether/ethyl acetate (2:3) v/v was used and obtained 83% yield.^{1}H NMR (CDCl$_3$,400 MHz). 7.12 (d, 2H, Ar-H) 7.49 (d, 2H,Ar-H) 9.26 (s, 1H, N-H) 3.68 (t, 4H, Pip-H) 2.46 (t, 4H, Pip-H) 2.4 (t, 2H, CH$_2$) 1.61 (t, 2H, CH$_2$) 8.35(s, 1H, C=N) 6.51 (d, 1H, Pyr-H) 6.15 (t,1H, Pyr-H) 6.95 (d, 1H, Pyr-H) 3.91(s,3H, CH$_3$) ^{13}C NMR: (400Hz, CDCl$_3$) 163.3(Ar-C) 115.8 (Ar-C) 131.0 (Ar-C) 134.1 (Ar-C) 57.1 (Pip-C) 56.7 (Pip-C) 62.1(CH$_2$) 47.1 (CH$_2$) 132.7 (Pyr-C) 124.8 (Pyr-C) 119.2 (Pyr-C) 110.9 (Pyr-C) 38.1(CH3) 153.7 (imine-C) 181.8 (sulfone-C) LCMS m/z Calculated for C$_{19}$H$_{24}$FN$_5$S:373.17,IR Vmax (cm-1) 3360 (N-H), 1670 (C=C), 1320 (C-N), 1690 (C=N) Elemental Analysis: Calculated C, 61.10; H, 6.48; F, 5.09; N, 18.75; S, 8.58,Experimental, C, 61.09; H, 6.47; F, 5.06; N, 18.72; S, 8.57.

2.2.2.10. (Z)-4-(2-(((1H-pyrrol-2-yl) methylene) amino) ethyl)-N-(4-bromophenyl) piperazine-1-carbothioamide(5j).

In column chromatography: solvent system petroleum ether/ethyl acetate (2:3) v/v was used and obtained 84% yield.^{1}H NMR (CDCl$_3$,400 MHz). 7.49 (d, 2H, Ar-H) 7.55 (d, 2H,Ar-H) 9.26 (s, 1H, N-H) 3.68 (t, 4H, Pip-H) 2.46 (t, 4H, Pip-H) 2.4 (t, 2H, CH$_2$) 1.61 (t, 2H, CH$_2$) 8.35(s, 1H, C=N) 6.51 (d, 1H, Pyr-H) 6.15 (t,1H, Pyr-H) 6.95 (d, 1H, Pyr-H) 3.91(s,3H, CH$_3$) ^{13}C NMR: (400Hz, CDCl$_3$) 122.7(Ar-C) 131.9 (Ar-C) 131.7 (Ar-C) 137.5 (Ar-C) 57.1 (Pip-C) 56.7 (Pip-C) 62.1(CH$_2$) 47.1 (CH$_2$) 132.7 (Pyr-C) 124.8 (Pyr-C) 119.2 (Pyr-C) 110.9 (Pyr-C) 38.1(CH$_3$) 153.7 (imine-C) 181.8 (sulfone-C) LCMS m/z Calculated for C$_{19}$H$_{24}$BrN$_5$S:433.09, IR V$_{max}$ (cm^{-1}) 3360 (N-H),), 1670 (C=C), 1320 (C-N), 1690 (C=N) Elemental Analysis: Calculated: C, 52.53; H, 5.57; Br, 18.39; N, 16.12; S, 7.38,Experimental; C, 52.51; H, 4.55; Br, 18.38; N, 16.10; S, 7.34.

2.2.2.11. (Z)-4-(2-(((1H-pyrrol-2-yl) methylene) amino) ethyl)-N-(4-iodophenyl) piperazine-1-carbothioamide(5k).

In column chromatography: solvent system petroleum ether/ethyl acetate (2:3) v/v was used and obtained 89% yield.^{1}H NMR (CDCl$_3$,400 MHz). 7.75 (d, 2H, Ar-H) 7.70 (d, 2H,Ar-H) 9.26 (s, 1H, N-H) 3.68 (t, 4H, Pip-H) 2.46 (t, 4H, Pip-H) 2.4 (t, 2H, CH$_2$) 1.61 (t, 2H, CH$_2$) 8.35(s, 1H, C=N) 6.51 (d, 1H, Pyr-H) 6.15 (t,1H, Pyr-H) 6.95 (d, 1H, Pyr-H) 3.91(s,3H, CH$_3$) ^{13}C NMR: (400Hz, CDCl^3) 86.5(Ar-C) 137.9 (Ar-C) 125.9 (Ar-C) 137.4 (Ar-C) 57.1 (Pip-C) 56.7 (Pip-C) 62.1(CH2) 47.1 (CH2) 132.7 (Pyr-C) 124.8 (Pyr-C) 119.2 (Pyr-C) 110.9 (Pyr-C) 38.1(CH$_3$) 153.7 (imine-C) 181.8 (sulfone-C) LCMS m/z Calculated for C$_{19}$H$_{24}$IN$_5$S: 481.08 ,IR V$_{max}$ (cm^{-1}) 3360 (N-H), 1670 (C=C), 1320 (C-N), 1690 (C=N) Elemental Analysis: CalculatedC, 47.41; H, 5.03; I, 26.36; N, 14.55; S, 6.66.Experimental; C, 47.38; H, 5.02; I, 26.34; N, 14.54; S, 6.63.
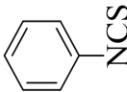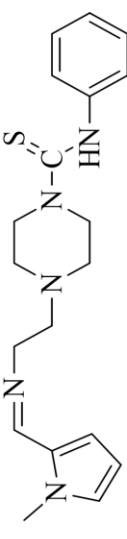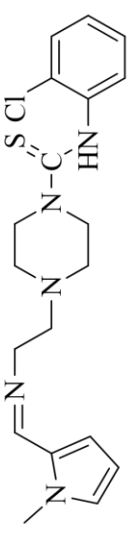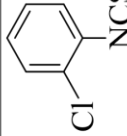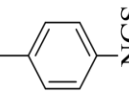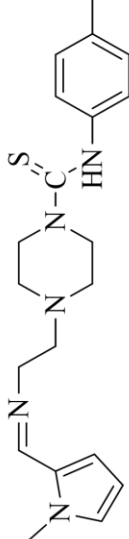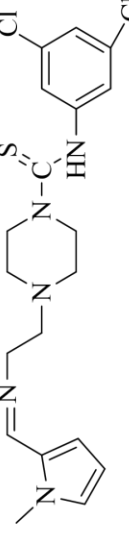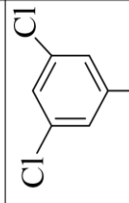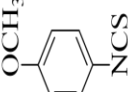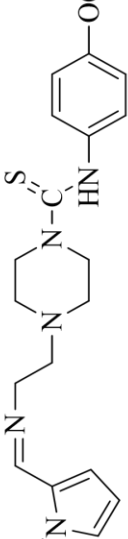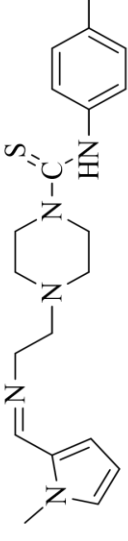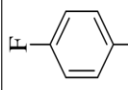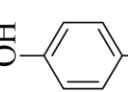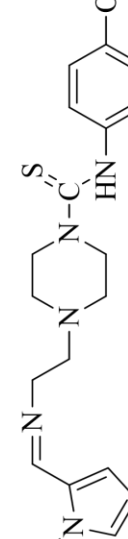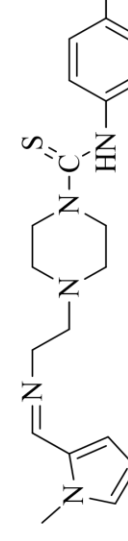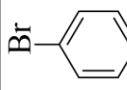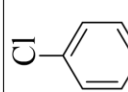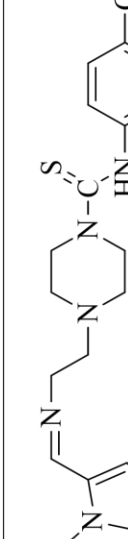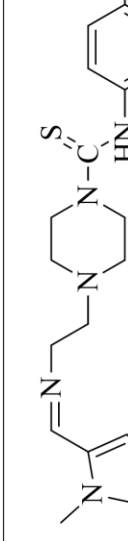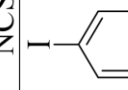
2.2.2.12. (Z)-4-(2-(((1H-pyrrol-2-yl) methylene) amino) ethyl)-N-(4-nitrophenyl) piperazine-1-carbothioamide(5l).

In column chromatography: solvent system petroleum ether/ethyl acetate (2:3) v/v was used and obtained 87% yield.^{1}H NMR (CDCl$_3$,400 MHz). 8.14 (d, 2H, Ar-H) 7.71 (d, 2H,Ar-H) 9.86 (s, 1H, N-H) 3.68 (t, 4H, Pip-H) 2.46 (t, 4H, Pip-H) 2.4 (t, 2H, CH$_2$) 1.61 (t, 2H, CH$_2$) 8.35(s, 1H, C=N) 6.51 (d, 1H, Pyr-H) 6.15 (t,1H, Pyr-H) 6.95 (d, 1H, Pyr-H) 3.91(s,3H, CH3) 13C NMR: (400Hz, CDCl$_3$) 86.5(Ar-C) 137.9 (Ar-C) 125.9 (Ar-C) 137.4 (Ar-C) 57.1 (Pip-C) 56.7 (Pip-C) 62.1(CH$_2$) 47.1 (CH2) 132.7 (Pyr-C) 124.8 (Pyr-C) 119.2 (Pyr-C) 110.9 (Pyr-C) 38.1(CH3) 153.7 (imine-C) 181.8 (sulfone-C) LCMS m/z Calculated for C$_{19}$H$_{24}$N$_6$O$_2$S 400.17,IR V$_{max}$ (cm^{-1}) 3360 (N-H), 1670 (C=C), 1320 (C-N), 1690 (C=N) Elemental Analysis: Calculated: C, 56.98; H, 6.04; N, 20.98; O, 7.99; S, 8.00,Experimental; C, 56.97; H, 6.03; N, 20.96; O, 7.95; S, 7.99.

2.3. Absorption, distribution, metabolism, and excretion (ADME) analysis and blood-brain barrier (BBB) permeability.

The suitability of a synthesized drug cannot be assessed only by its high potential but also by its good absorption, distribution, metabolism, and excretion. *In vitro*, ADME screens are available for a wide range of experimental techniques and high throughput. The free web tool Swiss ADME was used for this study. *In silico* ADME analysis helps to predict several significant aspects and is useful for analyzing the beneficial qualities of 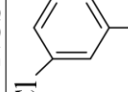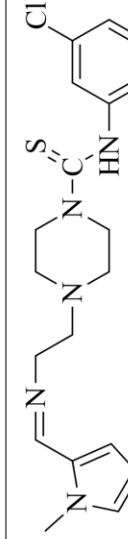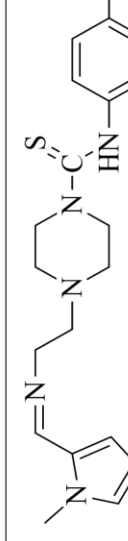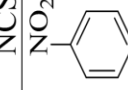compounds. Nowadays, computational ADME in conjunction with in vivo and in vitro predictions should be done as early as the drug discovery process because it decreases the number of safety issues [7]. According to Lipinski's rule, molecular features of a drug candidate are required to evaluate critical pharmacokinetic parameters such as ADME. Mol Inspiration, an online property calculation toolset accessible at http://www.molinspiration.com, was used to forecast ADME properties. It aids in designing and developing a possible therapeutic molecule [8]. Currently, the ADME property is in use. This is done utilizing a web tool to assess ADMET features such as aqueous solubility (log S), skin permeability (log Kp), synthetic accessibility score (SA), percentage absorption, pharmacokinetics, drug-likeness, and medicinal chemistry, as well as small molecule friendly properties [9]. The BBB permeability was evaluated by using the CB Ligand-BBB prediction server available at http://www.cbligand.org.

Table 1. Structure of synthesized compounds 5(a-l).

Comp. Name	R	Structure	Comp. Name	R	Structure
5a			5g		
5b			5h		
5c			5i		
5d			5j		
5e			5k		
5f			5l		

2.4. Prediction of activity spectra for test substances.

http://www.pharma expert.ru/PASS online/predict.php was used to predict the activity spectrum of computational screening of likely biological effects. This software created a technique for assessing an organic drug-like candidate's overall biological potential. PASS can predict the pharmacological impact, the molecular mechanisms of action, and the formation of unwanted side effects such as mutagenicity, teratogenicity, carcinogenicity, and embryotoxicity [10]. The PASS test will continuously predict the organic compound's biological activity based on its structure. Thus, before chemical production and biological testing, PASS can be used to evaluate the biological activity of virtual molecules [11].

2.5. Molecular docking validation.

A molecular docking simulation was run to examine the drug-target interactions of synthesized compounds with the help of Auto dock 4.2 software. All the chemical structures of compounds were drawn, and ChemDraw16.0 optimized their 3D architectures. A docking study examined the bind to the protein targets of S. aureus (6FTB), enabling Insilco docking simulations of the synthesized compounds' antibacterial activity. The protein data bank obtained the target proteins' X-ray crystallographic structure. Before the simulations, all bound ligands, co-factors, and water molecules were removed from the proteins. The Auto Dock atom types were defined using Auto Dock version 4.5, and Kollman charges were computed. The Auto Grid technique was used to build the three-dimensional grid boxes, and the grid maps reflecting the intact ligand in the actual docking target location were calculated. Finally, the binding free energy of a given inhibitor conformation in the macromolecular structure was calculated using Auto Dock. The default settings for the Lamarckian Genetic Algorithm (LGA) were 300 runs, 200 conformational possibilities, 100 populations, and 3,50,0000 energy evaluations. For each molecule, a maximum of 20 conformers were examined throughout the docking procedure. The results were evaluated based on the binding compatibility (binding energy) in kcal/mol and inhibition constant [12].

2.6. Antibacterial activity against MRSA.

2.6.1. MRSA culture preparation and maintenance.

The MRSA ATCC-43300 and *Staphylococcus epidermidis* ATCC-4990 were purchased from American Type Culture Collection. The single purified MRSA colony was inoculated into fresh Brain heart fusion (BHI) broth and incubated for 24 hours at 37° C. This was used in the entire experiment. The cell reading was adjusted to 0.5 according to the McFarland standard ($1x10^{-8}$ CFU/mL) with the help of UV-Vis spectroscopy at 600 nm [13]. 2.6.2. Minimum inhibitory concentration of pyrrole-coupled carbothioamide derivatives.

All the pyrrole-coupled carbothioamide derivatives were examined for MIC value by transferring sterilized BHI broth for each of 96 wells along with the various doses of synthesized derivatives (10-50μg/mL) dissolved in dimethyl sulfoxide (DMSO). Dispensed 10 μL of resazurin (270 mg in 40 mL of sterilized distilled water) indicator to all the wells. Finally, 10μL of MRSA bacterial culture (5×10^{6} CFU/mL) was seeded to achieve the culture density of 5×10^{5} CFU/mL. Streptomycin served as a standard bactericidal agent among broad-spectrum antibiotics. A mixture with all additions except the synthesized compound served as a positive control. The ones with all solutions without dispensing bacterial culture were negative controls. After being wrapped in thin plastic films, the plates are incubated at 37° C for 24 hours [14].

2.6.3. Disc diffusion method.

Out of the synthesized pyrrole-coupled carbothioamide derivatives (5a-l), based on the MIC value, compound 5d was chosen for studying the antibacterial activity by using the disc diffusion method in a dose-dependent manner. The MRSA culture was prepared from the young culture, and 1×10^7 CFU/mL cells were inoculated onto nutrient agar. The sterile 6 mm disc was placed on tryptone soya agar (TSA) and dispensed the different concentrations of 5d analog. Streptomycin (10μg/disc) was used as a standard antibacterial drug, and sterile saline water was used as a negative control. All the plates were incubated at 37° C for 24 h in an inverted position and recorded the zone of inhibition (ZOI) [15].

2.6.4. Validation of MRSA membrane damage.

2.6.4.1. MRSA bacterial cell membrane damage study by SEM.

The MRSA bacterial cell suspension was treated with double the MIC concentration of 5d for 2 h. The suspension was centrifuged at 5000 rpm, and the treated MRSA bacterial cells were fixed with phosphate buffer saline containing 2.5 % of glutaraldehyde. The fixed bacterial cells were washed with 30-100% ethanol incremental treatment. Finally, glass slides were air-dried at room temperature for 2 days and examined in a scanning electron microscope to observe the MRSAcell membrane damage [16].

2.6.4.2. Cell membrane damage analysis by measuring the cellular material leakage.

The MRSA bacterial cellular content leakage (DNA) was recorded in accordance with Chauhan and Kang. The MRSA bacterial culture was treated with double the MIC concentration of 5d and incubated at 37° C. The treated MRSA bacterial cell suspension was drawn at an interval of 0, 30, 60, 90, 120, and 150 min and centrifugated the suspension at 3500 rpm. The supernatant OD was measured at 260 nm in a UV-Vis spectrophotometer. All assays were performed in triplicate [17].

2.6.4.3.Cell membrane damage analysis by measuring the potassium efflux.

The MRSA bacterial cell membrane damage was further validated by changes in the potassium efflux according to the protocol of Wang. The overnight MRSA bacterial suspension was pelleted and re-suspended in 100 mM sodium phosphate buffer (pH 7). Next, the MRSA bacterial cell suspension was treated with a double MIC concentration of 5d in a 100 mL beaker and magnetically stirred at 30° C. The treated MRSA bacterial cell suspension was drawn at an interval of 0, 30, 60, 90, 120, and 150 min and centrifugated suspension at 3500 rpm. The potassium concentration was measured at 766.5 nm using ICP-OES (PerkinElmer, Optima-8000, and USA). The instrument was calibrated with 1–10 ppm NIST standards. All assays were performed in triplicate [18].

2.6.5. MRSA bacterial cell membrane damage study by electron transport chain (ETC).

2.6.5.1. Record of MRSA respiration by cyclic voltammogram.

The MRSA bacterial cell respiration was recorded by cyclic voltammogram in accordance with the method by Hassan and Wollenberger [19]. Before starting the experiment, the standard working electrode activated its electrochemical signals by dipping it in 0.1 M of

phosphate buffer of pH 7.0 and recording the cyclic scan in the range of 0.2 and 1.0 V with respect to 50 mV/S. The cyclic voltammogram (CV) was recorded at ambient temperature without stirring between 0.3 and 0.4 V with respect to 5 mV/S. All potential data was referred to as reference electrode Ag/AgCl / 3M KCl.

2.6.5.2. Measurement of the metabolic state of MRSA bacterial cells.

Initially, the metabolic activity of MRSA bacterial suspension was supplemented with 10 g/L of different carbon sources viz, D-(+)-galactose, D-(+)-glucose-succinate, and sodium acetate in sterile 0.1 M phosphate buffer (pH 7). After each carbon supplement, MRSA bacterial suspension was incubated at 37° C for 30 min. MRSA bacterial bio-electrochemical response was recorded compared to the control treated in the same manner but without carbohydrate supplementation [20].

2.6.5.3. Electro analysis.

The bio-electrochemical study was recorded with the help of an electrochemical instrument (Biologic Instruments SP-150). In this study, a set of electrodes viz, working (glassy carbon electrode (GCE)), auxiliary (platinum wire (Pt)), and reference electrodes (saturated calomel electrode (SCE) were used. GCE was first polished with 0.3-0.05 mm alumina slurry and washed with sterile water. Finally, the electrode was rinsed in ethanol, followed by sterile water for 2 min in sonication. The cyclic voltammograms were obtained at a scan rate of 10 mVs^{-1} in the potential range of 0.1-0.5 V [21].

2.6.6. MRSA respiration inhibition measurement after treatment with 5d analog.

The overnight MRSA culture suspension was centrifuged and washed with sterile PBS, and cell density was adjusted to 0.2 at A 600 nm. The bacterial respiration inhibition activity was measured by adding double the MIC concentration of 5d to a 50mL bacterial cell suspension in a constant temperature cup and stirred magnetically at 30°C. The bacterial respiration inhibition was assessed by comparing it with a control (without a sample) [22].

2.7. Study of MRSA-induced coagulation.

The anti-coagulation activity of the synthesized compound (5d) was studied on the coagulase-positive MRSA in accordance with the procedure in the Hi-media user manual. The 150 μL of previously reconstituted rabbit plasma in sterile saline water was mixed with 50 μL of different concentrations (25-250μg/mL) of 5d and 50 μL of overnight MRSA culture in Eppendorf tubes incubated at 37°C up to 4 h. The anti-coagulase activity was observed every hour, and data were recorded for clot formation by tilting tubes. Rabbit plasma alone and rabbit plasma with *Staphylococcus epidermises* were used as a reagent and negative control, respectively, and MRSA with rabbit plasma and Dabigatran drug as a positive and drug standard for comparison [23].

2.8. Anti-biofilm property of 5d.

The anti-biofilm activity of the synthesized 5d analog against MRSA was studied qualitatively and quantitatively in accordance with the method of Manu Kumar in sterile tissue culture plates [23]. In a sterile tissue culture plate containing 1500 mL of glucose-enriched

trypticase soy broth (TSB) and 100 L of overnight MRSA bacterial suspension, 50, 100, 150, and 200 g/mL of 5d samples were dispensed. For up to 18 hours, the tissue plate was incubated aerobically in a fixed condition at 37° C. After the biofilm maturation period, the tissue culture plate was washed with sterile phosphate buffer solution (PBS) and repeated to remove the planktonic bacterial cells. The biofilm developed from MRSA cells was fixed with the help of 500 µL of methanol for 20 min and allowed to air dry. Finally, adhered MRSA cells were stained with 0.5% crystal violet for 15 min and washed with PBS to remove the extra stains. The inhibition of biofilm was calculated based on the absorbance of eluted cells bound color in 1500 µL of 95% ethanol at 490 nm in a microplate spectrophotometer with negative control (only TSB medium). Assays were performed in triplicate.

2.9. Bio-compatibility.

2.9.1. RBC's hemolysis rate.

The synthesized compound (5d) at different concentrations (50, 100, 150, and 200 µg/mL) was added to freshly drawn sheep blood, incubated at 37°C for 30 min, and centrifuged at 3000 rpm for 5min. The absorbance of the supernatant was measured at 545 nm. The hemolysis rate (HR) was calculated using the below formula [24].HR=OD treated − OD negative control/OD positive control – OD negative control x100. Samples were considered highly hemocompatible if HR<5%, hemocompatible if HR<10%, and non-hemocompatible if HR > 20%.

2.10. Toxicity of synthesized analog.

2.10.1. Chemicals.

The cell line was procured from ATCC; stock cells were cultured in DMEM supplemented with 10% inactivated Fetal Bovine Serum (FBS), penicillin (100 IU/ml), streptomycin (100µg/mL) in a humidified atmosphere of 5% CO_2 at 37°C until confluent. The cell was dissociated with cell dissociating solution (0.2 % trypsin, 0.02 % EDTA, 0.05 % glucose in PBS). The viability of the cells was checked and centrifuged. Further, 50,000 cells /well were seeded in a 96-well plate and incubated for 24 hrs at 37°C, 5 % CO_2 incubator [25].

2.10.2. Preparation of test solutions.

For cytotoxicity studies, each weighed test drug was separately dissolved in DMSO. The volume was made up with DMEM supplemented with 2% inactivated FBS to obtain a stock solution of 1 mg/mL concentration and sterilized by filtration. Serial diluted synthesized analog was prepared at a concentration of 10 - 320 µg/mL for carrying out cytotoxic studies [26].

2.10.3. Determination of cell viability by MTT assay.

The monolayer cell culture was trypsinized, and the cell count was adjusted to 5 x 10^5 cells/ml using respective media containing 10% FBS. To each well of the 96-well microtiter plate, 100µL of the diluted cell suspension (50,000cells/well) was added. After 24 h, when a monolayer was formed, the supernatant was flicked off, washed the monolayer once with medium, and 100µLof different test concentrations of test drugs was added to the monolayer

in microtiter plates. The plates were then incubated at 37°C for 24hrs in a 5% CO_2 atmosphere. After incubation, the test solutions in the wells were discarded, and 100 µL of MTT (5mg/10ml of MTT in PBS) was added to each well. The plates were incubated for 4 h at 37°C in a 5% CO_2 atmosphere. The supernatant was removed,100µL of DMSO was added, and the plates were gently shaken to solubilize the formed formazan. The absorbance was measured using a microplate reader at a wavelength of 590 nm. The percentage growth inhibition was calculated using the following formula,

%   Inhibition = ((OD of Control – OD of sample)/OD of Control) x 100

and the concentration of test drug needed to inhibit cell growth by 50% (IC_{50}) values was generated from the dose-response curves for each cell line [27].

3. Results and Discussions

3.1. Pharmacophore model, ADME, and BBB analysis of synthesized compounds.

A molecule's pharmacological and pharmacokinetic properties are critical in making it a good therapeutic candidate. It is crucial to analyze a novel medicine's adsorption, distribution, metabolism, and excretion (ADME) and to assess conformity with Lipinski's criteria while designing a new drug. The pharmacophore model of the synthesized compound is shown in Figure 2.
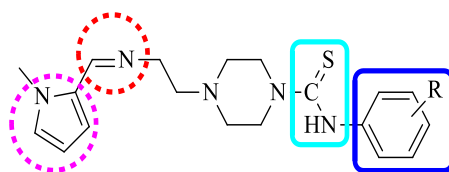
Figure 2. Pharmacophore model of synthesized compounds 5(a-l).
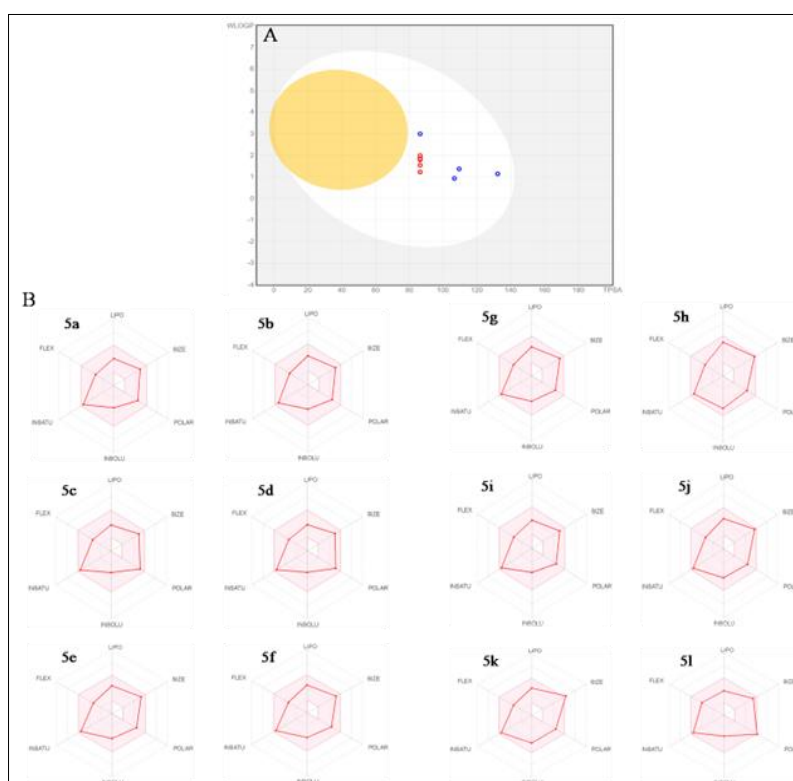
Figure 3. (**A**) The BOILED- Egg representation of GI and BBB properties of the compound 5(a-b); (**B**) Bioavailability radar graph of 5(a-l) (pink area reflects the allowed values of drug-likeness properties of the molecule.

According to Lipinski's rule, oral bioavailability drugs have no more than one violation of the following rules: There should be no more than 5 hydrogen bond donors. There should be no more than 10 hydrogen bond acceptors. The molecular weight (MW) of the substance is less than 500D. The pharmacophore model of synthesized compounds 5(a-l) pattern is represented in (Figure2). The calculated octanol-water partition coefficient (milogP) is<5. All the rules were followed by the synthesized piperazine molecule 5(a-l), as shown in Table 2. A compound could be a potential drug if a substance's topological polar surface area (TPSA) value is more than 140 and it has a lower oral bioavailability [28]. Table 2 displays the computed TPSA value for the produced physicochemical parameters such as H-acceptors, H-donors, and n-rotb. Figure 3 depicts synthesized molecules' gastrointestinal (GI) and blood-brain barrier (BBB) permeation properties. In this Figure 3A, the white region represents the physicochemical field of the molecule that can be absorbed by the gastrointestinal system, while the yellow region represents the physicochemical field of the synthesized compound that can penetrate the brain (Figure 3B). Using the formula % Abs = 109-0.345xTPSA, determined the percentage of absorption of the substances. The synthesized compounds (5a-l) have halogens which are electron-withdrawing groups, and OH, N-H, and C=S present in the compounds show good bioactive scores(Table 3). All the synthesized compounds show good BBB permeation except compounds 5c and 5l. Table 3 shows the expected Bioactivity score of synthesized analogs, which shows that compound 5dis a potent enzyme inhibitor and Kinase inhibitor [29].

Table 2.*In silico*c ores of physicochemical and pharmacokinetic parameters of the synthesized 5(a-l).

Sl no	miLog<5	H-Acceptors	H-Donors	Total polar Surface Area	n-rotb	Vio<1	MW <500	%ABS	BBB
5a	3.65	2	1	67.89	7	0	355.5	85.57	Yes
5b	3.82	2	1	67.89	7	0	369.53	85.57	Yes
5c	3.90	3	1	77.12	8	0	385.53	82.39	Yes
5d	3.17	3	2	88.12	7	0	371.5	78.59	Yes
5e	3.81	2	1	67.89	7	0	389.95	85.57	Yes
5f	3.87	2	1	67.89	7	0	389.95	85.57	Yes
5g	3.99	2	1	67.89	7	0	389.95	85.57	Yes
5h	4.04	2	1	67.89	7	0	424.39	85.57	Yes
5i	3.66	3	1	67.89	7	0	373.49	85.57	Yes
5j	3.84	2	1	67.89	7	0	434.4	85.57	Yes
5k	3.93	2	1	67.89	7	0	481.4	85.57	Yes
5l	3.38	4	1	113.71	8	0	400.5	69.77	No

Table 3. The bioactive score of the synthesized compound 5(a-l).

| Compound name	GPCR ligand	Ion channel modulator	Kinase inhibitor	Nuclear receptor ligand	Protease inhibitor	Enzyme inhibitor
5a	-0.24	-0.36	-0.13	-0.80	-0.72	-0.08
5b	-0.28	-0.42	-0.17	-0.80	-0.75	-0.14
5c	-0.27	-0.41	-0.16	-0.76	-0.72	-0.12
5d	-0.19	-0.30	-0.08	-0.63	-0.68	-0.03
5e	-0.24	-0.35	-0.14	-0.79	-0.73	-0.11
5f	-0.24	-0.35	-0.14	-0.80	-0.76	-0.13
5g	-0.27	-0.36	-0.11	-0.84	-0.79	-0.15
5h	-0.22	-0.32	-0.12	-0.76	-0.72	-0.12
5i	-0.23	-0.36	-0.09	-0.75	-0.71	-0.10
5j	-0.33	-0.42	-0.17	-0.88	-0.81	-0.15
5k	-0.23	-0.34	-0.11	-0.74	-0.76	-0.13
5l	-0.36	-0.36	-0.26	-0.80	-0.77	-0.17

3.2. Synthesis and characterization.

In the present study, pyrrole-based carboxamide derivatives of (Z)-4-(2-((1-methyl-1H-pyrrol-2-yl) methylene) amino) ethyl)-N-phenylpiperazine-1-carbothioamide (5a-1) were synthesized (Figure 1). The structure of synthesized compounds was tabulated in Table 1. The structure of produced substances was determined by spectral studies. It's a single-step process involving 1-methyl-1H-pyrrole-2-carbaldehyde (1) and 2-(piperazin-1-yl) ethane-1-amine (2) were used to synthesize the compound (Z) N-(2-(piperazin-1-yl) ethyl) methanimine -1-(1-methyl-^{1}H-pyrrol-2-yl)-N-(2-(piperazin-1-yl) ethyl) methanimine (3). We examined compound (3) with a different spectral approach. Compound(3) FT-IR spectra bands at 3300 cm^{-1} indicate the presence of an NH group, whereas a peak at 1620 cm^{-1} indicates the presence of C=N moieties. The molecular ion peak (m/z) of compound (3) is 220.17, whereas ^{1}H-NMR spectra show a singlet peak at 3.91, shows the presence ofN-CH$_3$ proton, and singlet peak at 8.28, indicating the presence of imine proton. These spectrums confirm the structure of the compound (3). The series of analogs 5a-l, (Z)-4-(2-(((1-methyl-1H-pyrrol-2-yl) methylene) amino) ethyl)-N-phenylpiperazine-1-carbothioamide (5a-1) were synthesized using(Z)-1-(1-methyl-1H-pyrrol-2-yl)-N-(2-(piperazin-1-yl) ethyl) methanimine and substituted isothiocyanatobenzene as shown in Figure 1. Evaluation of synthesized series of analogs 5a-5l by various spectral methods, FT-IR spectra of all compounds recorded within range of 4000-400 cm^{-1}. The C=N group possesses strong absorption bands at 1550 cm^{-1}, the N-H stretch has a band at 3431 cm^{-1}, and the -CH$_2$ rocking band at 750 cm^{-1}. CDCl$_3$ was used to report the synthesized compounds' distinctive peaks of resonance in 1H-NMR and ^{13}C NMR. They were given the resonance based on their peak multiplicity and integration. The integration spectra of the newly synthesized compounds were in good accordance with the integration spectra. The ^{1}H-NMR spectra of synthesized compounds 5d exhibit a single peak at 8.28, assigned to the CH=N proton, and a singlet peak at 3.91, ascribed to the N-CH$_3$ proton. The pyrrole protons are indicated by two doublet peaks at 7.15 and 6.79, as well as a triplet peak at 6.22. A triplet peak shows the piperazine protons at 2.48 and 3.39. Aromatic protons also produce a doublet peak to appear between 7.37 to 8.17. The ^{13}C NMR spectra for 5a-5l indicated that the groups were in the range of 38.1-155.1ppm. The observed molecular ion peak value in the mass spectra of compounds 5a-5l is in good arrangement with the molecular formula of produced compounds. All the spectra of synthesized compounds are shown in Supplementary Figures 1-9.

3.3. Biological activity spectrum PASS analysis.

The PASS software is a free web application that may be used to determine synthetic analogues' biological activity spectrum, and it was used to determine the activity of the synthesized compounds [30]. All the synthesized compounds exhibit Pa (probable activity) values greater than Pi(probable inactivity) for the activities, Chemo sensitizer, Histone deacetylase stimulant, Antineoplastic (pancreatic cancer), Polarization stimulates, Antiprotozoal (Amoeba), Protein kinase (ck1) epsilon inhibitor, Cytidine deaminase inhibitor, Antineoplastic (lung cancer), Autotoxin inhibitor. The pa and pi values of the produced molecules are excellent, and it represents the therapeutic agent's potential in the future. The PASS values of the synthesized compounds are tabulated in the supplementary table S1. The compound 5d shows potent values of Pa value 0.585 and Pi value of 0.008 for the Chemo sensitizer activity, for Histone deacetylase stimulant activity Pa value of 0.465 and Pi value of 0.003; for Polarization stimulates activity, Pa value of 0.804 and Pi value 0.002, for Antiprotozoal (Amoeba) activity Pa value 0.303 and Pi value 0.066 for Protein kinase (ck1) epsilon inhibitor activity Pa value 0.173 and Pi value 0.052 for Cytidine deaminase inhibitor activity Pa value 0.183 and Pi value 0.028 for Antineoplastic (lung cancer) activity PA value 0.166 and Pi value 0.088 for Autotoxin inhibitor activity Pa value 0.203 and Pi value 0.003. The excellent Pa and Pi values of the synthesized compounds 5d suggest that they could be utilized as futuristic therapeutic agents. Pa and Pi values of synthesized compound 5(a-l) were tabulated in supplementary table S1.

3.4. Molecular docking studies.

In the field of medicinal chemistry, molecular docking is a very useful technology in computational chemistry that has played a critical role in drug discovery and design. The binding region and interaction of a compound within the binding site of a receptor protein are investigated using molecular docking methods. The *in silico* molecular docking computational method was utilized to validate this, providing an effective way of laying the fundamental foundation for drug discovery to treat deadly cancer. By choosing protein 6FTB from the RCSB protein data bank [31], this *in silico* approach was applied to examine the dynamics of biological interactions. Compound 5d shows a high docking score of -6.95 with 6FTB (Table 4). The active binding site of compound 5d with respect to protein 6FTB is shown in Figures 4A and 4C; the compound 5d demonstrated Vander Waals interactions with GLY A: 130, VAL A: 128, GLY A: 131, GLN A: 129, LEU A: 119, THR A: 115, Conventional hydrogen bond with M A: 0E301, M A: 0E303, carbon-hydrogen bond with PO A: 4313 in 6FTB protein, due to this interactions compound 5d exhibit high docking score with good binding energy. In this study, the 5d has a good docking score compared to other analogs, and also this theoretical data strongly correlated to our experimental results. The docking score and binding interaction of all synthesized compounds were tabulated in Supplementary Table S2 and Table S3, respectively.
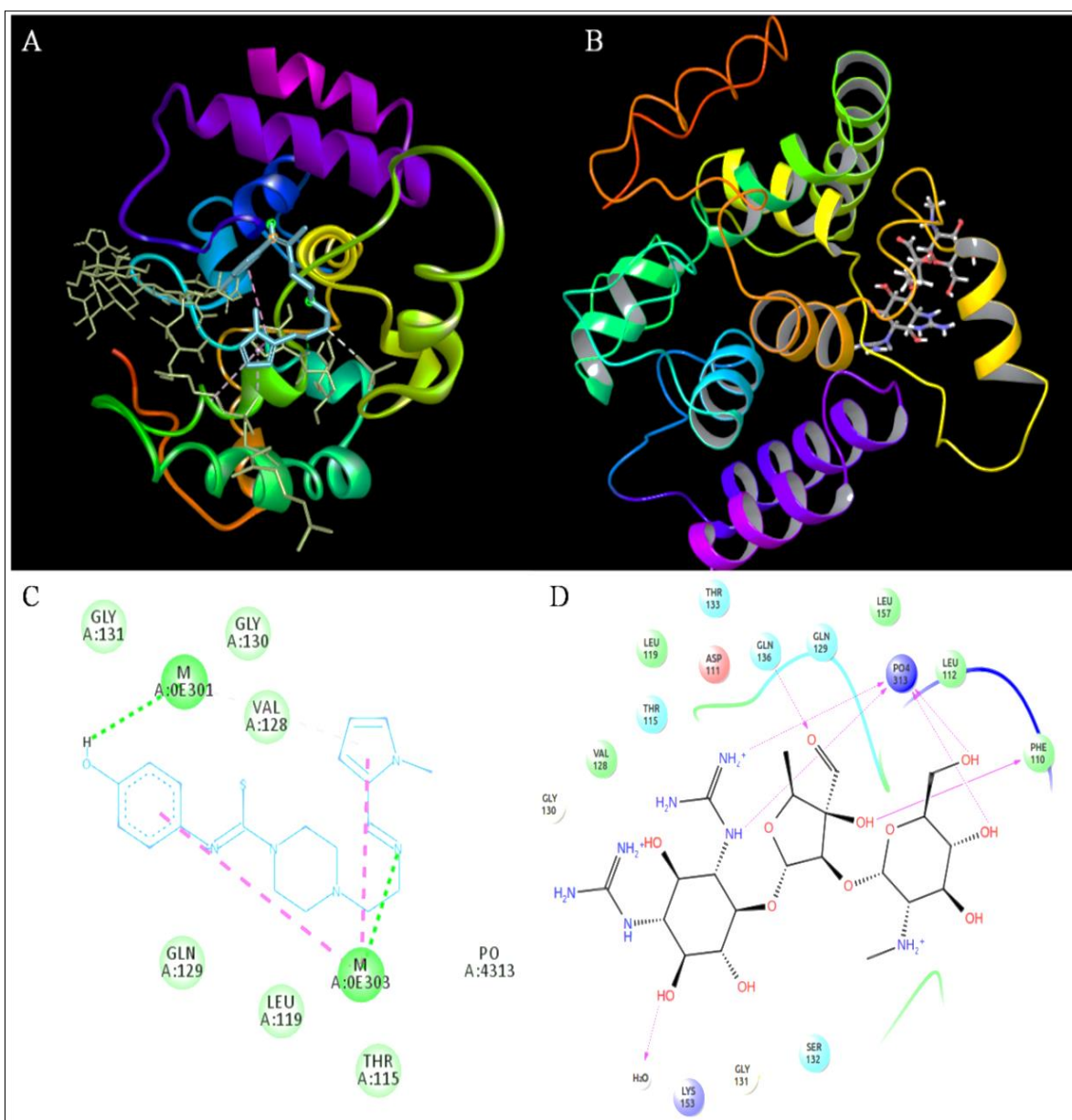
Figure 4. (**A & C**) Molecular docking interactive map of molecule 5dfor 6FTB and (**B&D**) antibiotic streptomycin of binding deep inside the active site, depicting the best docking pose showing 3D and 2D, respectively.

Table 4. Molecular docking results for the compound 5d and receptor (PDB ID: 6FTB).
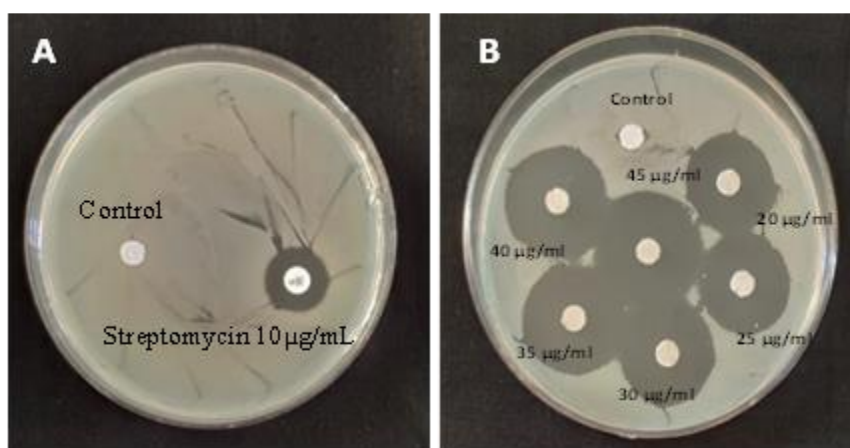
Protein id	Compound Name	Binding Score
6FTB	5d	-6.95
	Streptomycin	-7.56

3.5. Antibacterial activity.

The antibacterial activity of pyrrole-coupled carbothioamide derivatives 5(a-l) revealed good pharma-core characteristics and ADME activity. The various concentration of 5(a-l) (10-100 µg/mL) was used to estimate the minimum inhibitory concentration against perilous MRSA culture, and data was tabulated in Table 5. The pyrrole-coupled carbothioamide derivative5d exhibited effective antibacterial action compared to standard antibiotic streptomycin (16.10±0.06mm Zone of inhibition (ZOI)) at 10 µg/disc against MRSA in a dose-dependent manner (20, 25, 30, 35, 40 &45 µg/mL) with ZOI of 17.10±0.05, 17.9±0.04, 18.40±0.06, 18.90±0.04, 19.10±0.08, and 19.90±0.04 in mm respectively (Figure 5A and 5B). The shown data shows slightly higher antibacterial activity compared to 5e, 5f, and 5g due to

the electron-donating group in the phenyl ring. The compound 5dreleased that electron-donating hydroxyl functionalized derivatives presented relatively good antibacterial activity.

Table 5. Antibacterial activity of the synthesized pyrrole coupled carbothioamide derivatives5(a-l) against methicillin-resistant *Staphylococcus aureus* (MRSA).

Pyrrole coupled carbothioamide derivatives (5a-l)	MIC in µg/mL
5a	50±0.30
5b	54±0.50
5c	58±0.20
5d	18±0.20
5e	24±0.40
5f	28±0.40
5g	46±0.20
5h	54±0.10
5i	42±0.30
5j	40±0.20
5k	56±0.50
5l	58±0.30
Streptomycin	10 µg

Figure 5. Antimicrobial activity 5d against MRSA. (**A**) MRSA tested with standard drug streptomycin10µg/disc (16.10±0.06) ZOI in mm. (**B**) 5d with different concentrations ranging from 20, 25, 30, 35, 40 & 45 µg/mL (17.10±0.05, 17.9±0.04, 18.40±0.06, 18.90±0.04, 19.10±0.08, and 19.90±0.04ZOI in mm respectively).

3.6. Membrane damage study.

3.6.1. MRSA membrane cell damage by SEM, cellular leakage, and potassium efflux.

The antibacterial activity of 5d was further validated by studying the membrane damage of MRSA bacterial cells. Overnight MRSA bacterial cell suspension was treated twice the MIC of 5d and without the synthesized analog, considered a control. The MRSA cell surface showed significant membrane changes, such as pores, misshapes, and cracks, compared to the untreated control by SEM (Figures 6A and 6B). Additionally, the cell membrane damage of MRSA was confirmed by quantifying potassium efflux variation and cellular content leakage (DNA) during cell damage. The revealed result showed an increase in the leakage of cellular content and potassium content in the solution with respect to an increased dose of 5d. This is mainly because of damage to the cell membrane of MRSA (Figures 7A &7B).
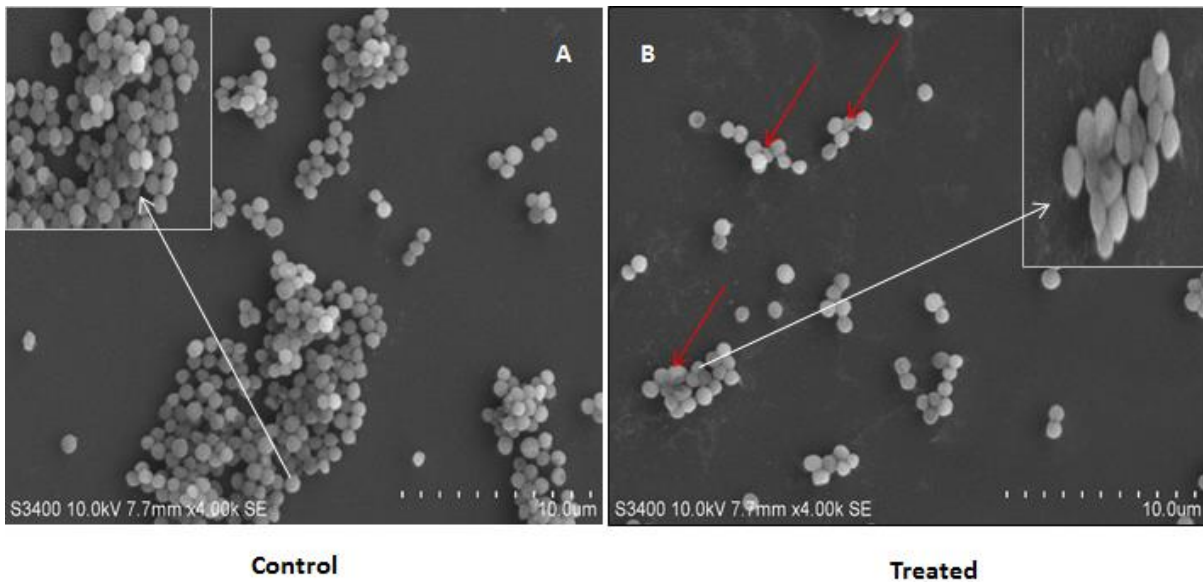
Figure 6. Antibacterial activity of 5d was demonstrated by cell membrane damage of MRSA.
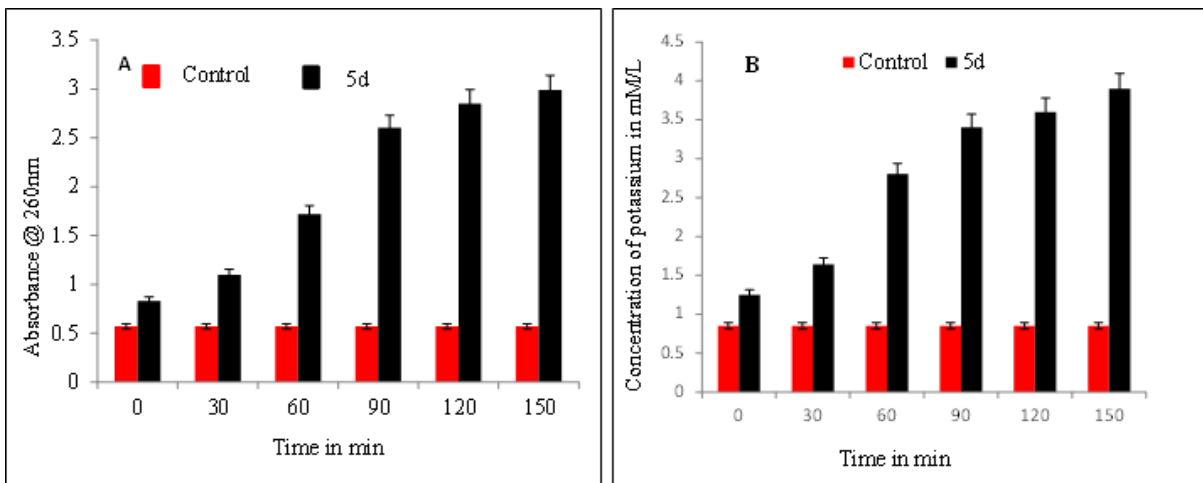
Figure 7. (A) MRSA cell membrane damage assay validated by cellular content (DNA) leakage and **(B)** Measurement of potassium content in suspension after treated with 5e.

3.7. Study of MRSA respiration by measuring cyclic voltammogram (CV).

The antibacterial efficacy of 5d was confirmed by the increase of holes in MRSA bacterial cell membranes with the help of a cyclic voltammogram (CV).
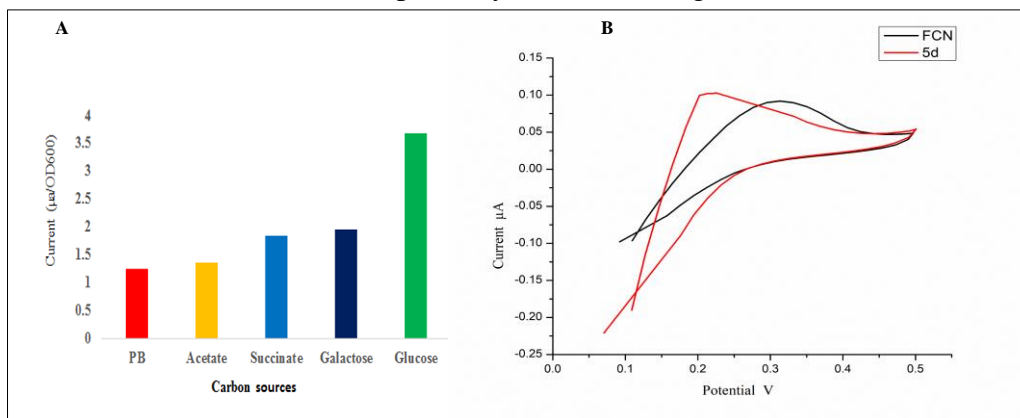
Figure 9. The cyclic voltammogram (CV) measurement. **(A)** Measurement of current in µA after the treatment of MRSA cell suspension response to FCN/DCPIP with respect to carbon source glucose (10g/L) in presence and absence mode. **(B)** Treatment of MRSA cell suspension with 1mM ferric cyanide (FCN) and measurement of current in µA after the treatment of MRSA cell suspension with 5d analog in the presence of ferric cyanide.

In addition, the differences in the MRSA cells' bio-electrochemical results in the ETC (electron transport chain) were recorded. Before starting the CV measurement, MRSA bacterial cell suspension was grown in the presence of a glucose carbon source, and their CV was 0.200A–0.4989V (9A).

The ferric cyanide (FCN) showed a weak response to the MRSA cell membrane crossing barrier with a score of (0.2984 A at 0.4923V) compared to the 2, 6-Dichlorophenolindophenol (DCPIP) with a strong signal having a score of (0.3783 A at 0.2950V). In addition to this, a double-mediated protocol was established for FCN-DCPIP (0.2945 A at 0.7854V), which showed a substantial rise in the electrical response(Supplementary Figures S10 A and B). In the experience of this prominence, treatment of the MRSA culture with 5d was seen to elicit an electrical response. This is comparable to that of FCN, suggesting its ability to cause a substantial cell membrane damaging effect in the bacterial culture (0.5020Aat0.2030V) (Figure 9A and 9B).

3.8. The anti-coagulase activity of 5d.

The anti-coagulation test was executed to verify the coagulation prevention efficacy of 5d against MRSA coagulase in comparison with the well-known standard anti-coagulant drug Dabigatran (Pradaxa) by using rabbit plasma. In this summary, 5d showed inhibition of coagulation by inhibiting the conversion of soluble fibrinogen to insoluble fibrin (creamy white clot) in rabbit plasma at a 25 µg/mL concentration. The result was confirmed with the well-known standard drug Dabigatran, which effectively inhibited the coagulation formation in rabbit plasma at a low concentration of 10µg/mL (Figure 8).
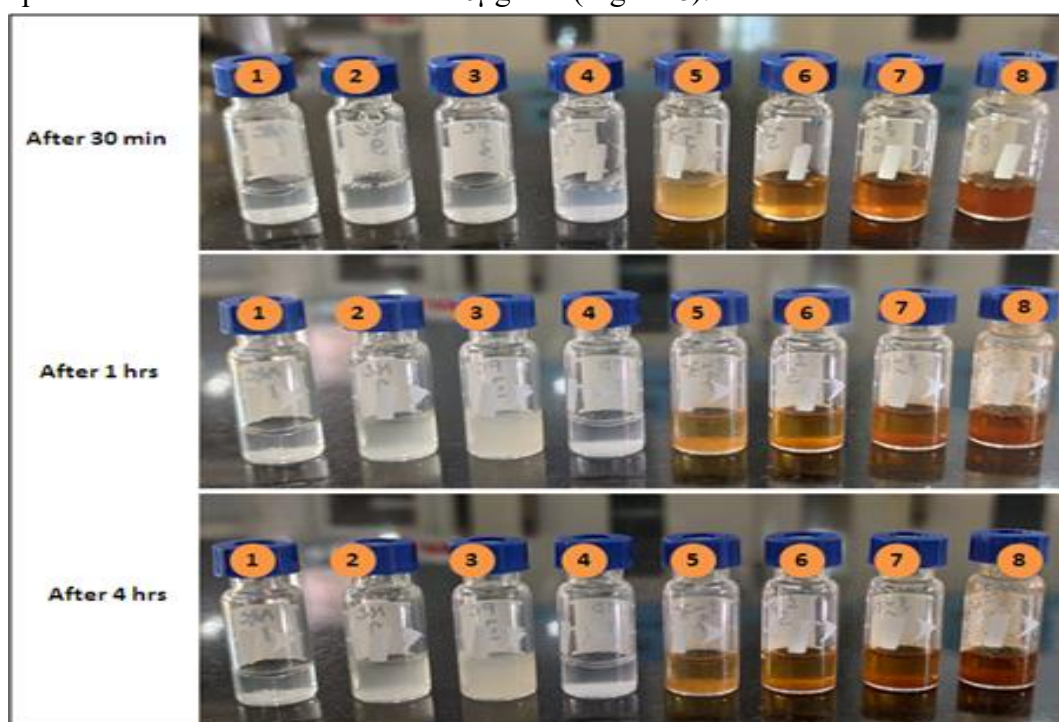

Figure 8. The images represent the anti-coagulation activity of 5d. The Eppendorf tube 1 was reagent control (only rabbit plasma), 2 rabbit plasma mixed with 50µL of *S. epidermises* culture as a negative coagulase reaction, 3 rabbit plasma with MRSA culture, 4 rabbit plasma with 10 µg/mL standard drug Dabigatran and from 5 to 8 rabbit plasma and MRSA culture with different concentrations of 5d. All the glass autosampler vials were incubated at 37ºC for up to 4 hrs. The images were taken 30 min, 1 hr, and 4 hours after the reaction of the experiment. This image showed no clot in the reagent, negative control, clot formation in the positive control (untreated), and clot inhibition in the Dabigatran drug at 10µg/mL. The **5d** sample showed that it inhibited the fibrin formation at 25 µg/mL.

3.9. Antibiofilm activity of 5d against sessile MRSA.

In MRSA biofilms, cells have been embedded in an extracellular polymeric matrix and form aggregates attached to an abiotic or biotic surface or non-attached are known as biofilms (free-floating aggregates). In this environment, the metabolism, gene transcription, and protein expression between planktonic cells and cells in biofilms show striking variations. Strong biofilms created by MRSA can cause serious infections resistant to antibiotics, most commonly in diabetic patients with chronic skin ulcers and fresh burn wounds.
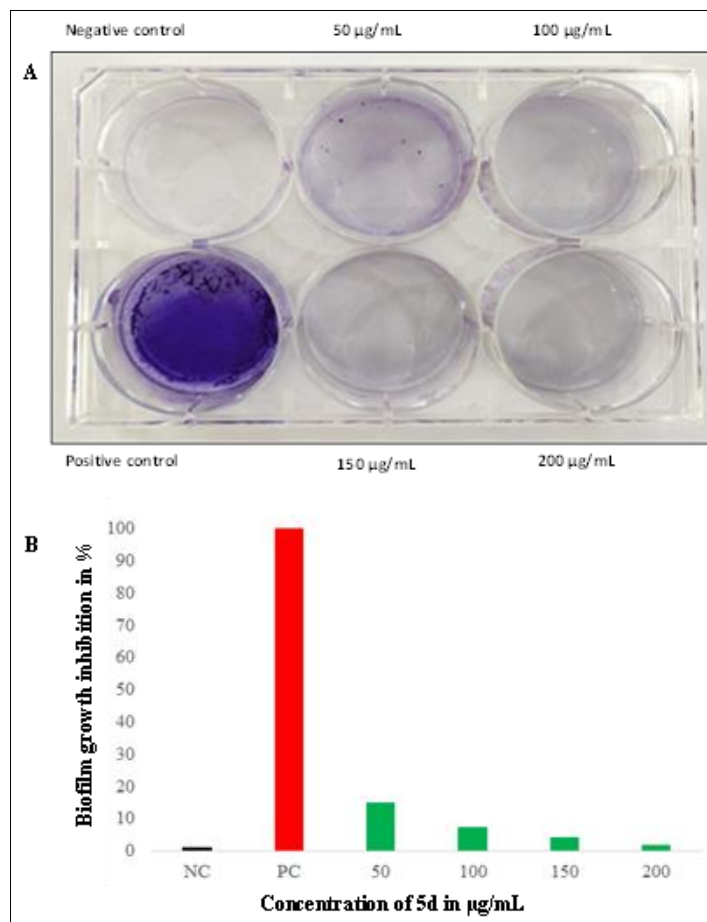
Figure 9. Antibiofilm activity of 5d. (**A**)Qualitative antibiofilm activity of the crystal violet dye method and (**B**) Quantitative antibiofilm inhibition.

3.10. Biocompatibility study.

To report the safety of synthesized 5d analog's reaction in the bloodstream, it is necessary to assess the RBCs biocompatibility and found 5d did not alter the erythrocytes membrane up to the concentrations of 750 µg/mL. Generally, in some medicines, due to an imbalance of osmotic pressure in the bloodstream, RBCs release the hemoglobin content by lysis. In this scenario, 5d analog addressed the compatibility without altering the RBCs in the biological domain with excellent blood biocompatibility and a suitable contender to minimize the MRSA infection by acting as potent anti-staphylococcal property (10A, B, & C).

3.11. Toxic effect of analog 5d.

In the current investigation, the potential 5d compound was tested for cytotoxicity against 3T3-L1 cell lines by MTT assay with different dose manners to check the antiproliferative effect. We had chosen the **5d** compound for the cytotoxicity assay because it

was found to be a very potential contender against MRSA. The revealed data indicated that the synthesized **5d** analog showed an IC_{50} value of 357.50 µg/mL compared to the standard drug Doxorubicin 28.21µM (Figures 11& 12).
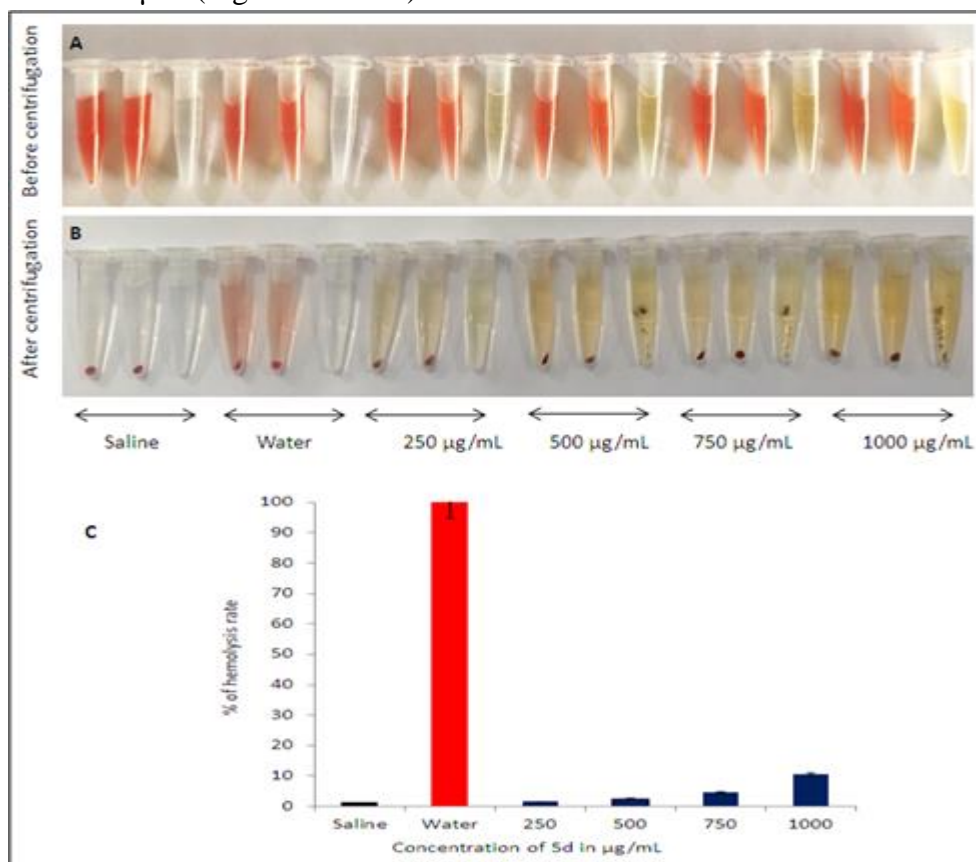
Figure 10. The blood biocompatibility assay.
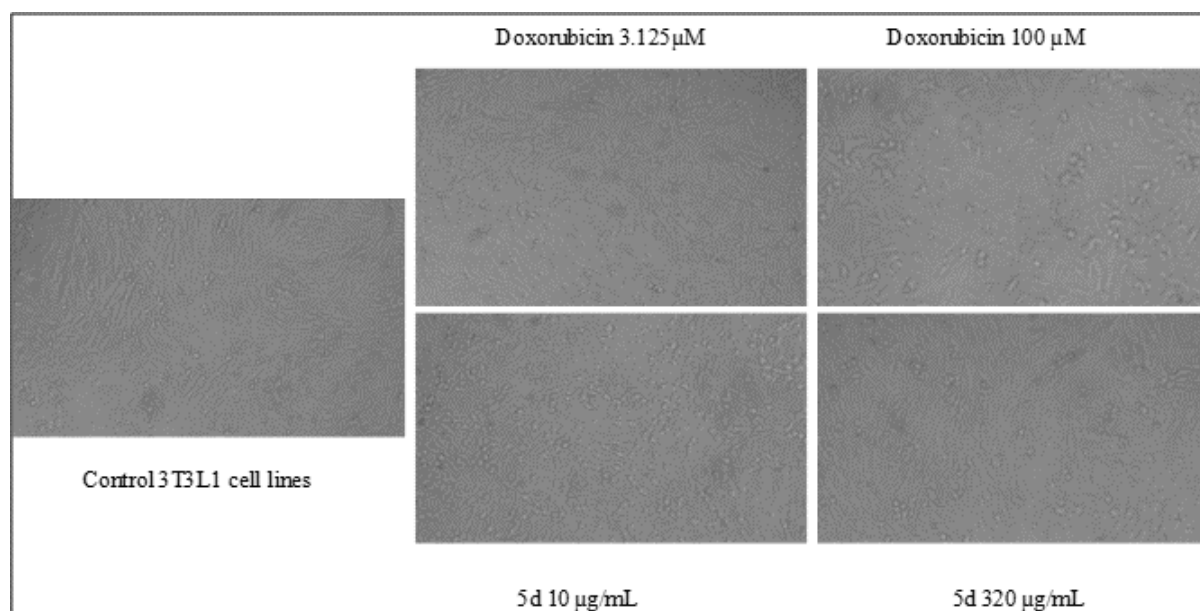
Figure 12. % Inhibition of 3T3-L1 cells with different concentrations of Doxorubicin and 5d.

4. Conclusions

In this study, we designed and synthesized the various pyrrole-coupled carbothioamide derivatives 5(a-l) as a probable antibacterial agent against MD-MRSA. All the derivatives were amply characterized by various methods. The nature of drug-likeness was examined

meticulously by pharmacophore, ADME, and BBB. The antibacterial effectiveness of the synthesized drug was validated with in-vitro techniques viz., MRSA bacterial cell membrane damage by SEM images, measurement of cellular material content leakage (DNA), potassium efflux, and inhibition of bacterial respiration. In addition, anti-MRSA activity was again theoretically validated by an *in silico* docking study on the protein 6FTB of MRSA, which showed a good docking score and binding energy. The 5d analog showed good biocompatibility and was less toxic to normal cell lines. Based on the obtained results, we conclude that further fine-tuning of the 5d compound will have tremendous therapeutic applications for bacteremia, endocarditis, sepsis, and scaled skin infections caused by MRSA.

Funding

Acknowledgments

Conflicts of Interest

We declare that we have no conflict of interest.

References

1. Zheng, Y.; Wang, Z.; Liu, C.; Tao, L.; Huang, Y.; Zheng, Z. Integratedproduction of aromatic amines, aromatic hydrocarbon and N-heterocyclic bio-char from catalytic pyrolysis of biomass impregnated with ammonia sources over Zn/HZSM-5 catalyst. *Journal of the Energy Institute***2020**, *93*, 210-223,https://doi.org/10.1016/j.joei.2019.03.007.

2. Motati, D. R.; Amaradhi, R.; Ganesh, T. Recent developments in the synthesis of azaindoles from pyridine and pyrrole building blocks. *Organic Chemistry Frontiers***2021**,*8*, 466-513,https://doi.org/10.1039/D0QO01079K.

3. Zong, P.; Jiang, Y.; Tian, Y.; Li, J.; Yuan, M.; Ji, Y.; Qiao, Y. Pyrolysis behavior and product distributions of biomass six group components: Starch, cellulose, hemicellulose, lignin, protein and oil. *Energy Conversion and Management***2020**,*216*, 112777,https://doi.org/10.1016/j.enconman.2020.112777.

4. Shaibuna, M.; Theresa, L. V.; Sreekumar, K. A new green and efficient brønsted: Lewis acidic DES for pyrrole synthesis. *Catalysis Letters***2018**,*148*, 2359-2372,https://doi.org/10.1007/s10562-018-2414-4.

5. Lin, Z. Q.; Li, C. D.; Zhou, Z. C.; Xue, S.; Gao, J. R.; Ye, Q.; Li, Y. J. Copper (II)-promoted oxidation/[3+2]cycloaddition/aromatizationcascade: efficient synthesis of tetrasubstituted NH-pyrrole from chalcones and iminodiacetates. *Synlett***2019**, *30*, 1442-1446,https://doi.org/10.1055/s-0039-1689972.

6. Nataraj, B. H.; Mallappa, R. H. Antibiotic resistance crisis: an update on antagonistic interactions between probiotics and methicillin-resistant Staphylococcus aureus (MRSA). *Current Microbiology***2021**, *78*, 2194-2211,https://doi.org/10.1007/s00284-021-02442-8.

7. El-Serwy, W. S.; El-Serwy, W. S.; Mohamed, N. A.; Kassem, E. M.; Mostafa, R. E.; Mohamed, H. S. Synthesis, Biological Evaluation, Molecular Docking, ADME Predictions and QSAR Studies of Novel 1, 2-Diazet and Pyrrole Derivatives as Anti-Inflammatory Agents. *Russian Journal of Bioorganic Chemistry***2021**,47, 183-198,https://doi.org/10.1134/S1068162021010040.

8. Khizr, M.; Sahoo, S. C.; Khan, M. M. Synthesis, characterization, X-ray crystallographic study and *in silico* ADME predictions of functionalized nitropyrrole derivatives. *Journal of Molecular Structure***2022**,*1250*,131655,https://doi.org/10.1016/j.molstruc.2021.131655.

9. Kaur, M.; Singh, P. Targeting Tyrosine kinase: Development of acridone–pyrrole–oxindole hybrids against human breast cancer. *Bioorganic & Medicinal Chemistry Letters* **2019**, *29*, 32-35, https://doi.org/10.1016/j.bmcl.2018.11.021.

10. Oliveira, N. J. C.; Teixeira, I. N. S.; Fernandes, P. O.; Veríssimo, G. C.;Valério, A. D.; de Souza Moreira, C. P.; de Oliveira, R. B. Computer-aided molecular design, synthesis and evaluation of antifungal activity of heterocyclic compounds. *Journal of Molecular Structure* **2022**, *1267*, 133573, https://doi.org/10.1016/j.molstruc.2022.133573.

11. Khan, T.; Ahmad, R.; Azad, I.; Raza, S.; Joshi, S.; Khan, A. R. Computer-aided drug design and virtual screening of targeted combinatorial libraries of mixed-ligand transition metal complexes of 2-butanone thiosemicarbazone. *Computational biology and chemistry* **2018**, 75, 178-195, https://doi.org/10.1016/j.compbiolchem.2018.05.008.

12. Azad, I.; Jafri, A.; Khan, T.; Akhter, Y.; Arshad, M.; Hassan, F.; Nasibullah, M. Evaluation of pyrrole-2, 3-dicarboxylate derivatives: Synthesis, DFT analysis, molecular docking, virtual screening and *in vitro* anti-hepatic cancer study. *Journal of Molecular Structure* **2019**, *1176*, 314-334, https://doi.org/10.1016/j.molstruc.2018.08.049.

13. Kang, S.; Kong, F.; Liang, X.; Li, M.; Yang, N.; Cao, X.; & Zheng, Y. Label-free quantitative proteomics reveals the multitargeted antibacterial mechanisms of lactobionic acid against methicillin-resistant Staphylococcus aureus (MRSA) using SWATH-MS technology. *Journal of agricultural and food chemistry* **2019**, *67*, 12322-12332, https://doi.org/10.1021/acs.jafc.9b06364.

14. Boudjellal, F.; Ouici, H. B.;Guendouzi, A.;Benali, O.; Sehmi, A. Experimental and theoretical approach to the corrosion inhibition of mild steel in acid medium by a newly synthesized pyrazole carbothioamide heterocycle. *Journal of Molecular Structure* **2020**, *1199*, 127051, https://doi.org/10.1016/j.molstruc.2019.127051.

15. Mathi, D. B.; Gopi, D.; Kavitha, L. Implication of lanthanum substituted hydroxyapatite/poly (n-methyl pyrrole) bilayer coating on titanium for orthopedic applications. *Materials today: proceedings* **2020**,*26*, 3526-3530, https://doi.org/10.1016/j.matpr.2019.06.152.

16. Peixoto, P.; Guedes, J. F.; Rombi, E.; Fonseca, A. M.; Aguiar, C. A.; Neves, I. C. Metal ion–zeolite materials against resistant bacteria, MRSA. *Industrial & Engineering Chemistry Research* **2021**, *60*, 12883-12892, https://doi.org/10.1021/acs.iecr.1c01736.

17. Kang, S.; Kong, F.; Shi, X.; Han, H.; Li, M.; Guan, B.; Yue, X. Antibacterial activity and mechanism of lactobionic acid against Pseudomonas fluorescens and Methicillin-resistant Staphylococcus aureus and its application on whole milk. *Food Control* **2020**, *108*, 106876, https://doi.org/10.1016/j.foodcont.2019.106876.

18. Lee, W.; Lee, D. G. Potential role of potassium and chloride channels in regulation of silymarin-induced apoptosis in Candida albicans. *IUBMB life* **2018**,*70*, 197-206, https://doi.org/10.1002/iub.1716.

19. Hsueh, A. J.; Park, S.; Satoh, T.; Shimizu, T.; Koiwai, K.; Nakashima, M.; Suzuki, H. Microdevice with an Integrated Clark-Type Oxygen Electrode for the Measurement of the Respiratory Activity of Cells. *Analytical Chemistry* **2021**, *93*, 5577-5585, https://doi.org/10.1021/acs.analchem.1c00227.

20. Sarkar, P.; Basak, D.; Mukherjee, R.; Bandow, J. E.; Haldar, J. Alkyl-Aryl-Vancomycins: Multimodal Glycopeptides with Weak Dependence on the Bacterial Metabolic State. *Journal of Medicinal Chemistry* **2021**,*64*, 10185-10202, https://doi.org/10.1021/acs.jmedchem.1c00449.

21. Pathare, N. A.; Asogan, H.; Tejani, S.;Al Mahruqi, G.; Al Fakhri, S.; Zafarulla, R.; & Pathare, A. V. Prevalence of methicillin resistant Staphylococcus aureus [MRSA] colonization or carriage among healthcare workers. *Journal of Infection and Public Health* **2016**, *9*, 571-576, https://doi.org/10.1016/j.jiph.2015.12.004.

22. Schoeffel, J.; Wang, E. W.; Gill, D.; Frackler, J.; Horne, B. A.; Manson, T.; Doub, J. B. Successful Use of Salvage Bacteriophage Therapy for a Recalcitrant MRSA Knee and Hip Prosthetic Joint Infection. *Pharmaceuticals* **2022**,*15*, 177, https://doi.org/10.3390/ph15020177.

23. Lee, W. R.; Hsiao, C. Y.; Huang, T. H.; Sung, C. T.; Wang, P. W.; Cheng, W. T.; Fang, J. Y. Low-fluence laser-facilitated platelet-rich plasma permeation for treating MRSA-infected wound and photoaging of the skin. *International Journal of Pharmaceutics* **2021**, *595*, 120242, https://doi.org/10.1016/j.ijpharm.2021.120242.

24. Podsiedlik, M.; Markowicz-Piasecka, M.; Sikora, J. Erythrocytes as model cells for biocompatibility assessment, cytotoxicity screening of xenobiotics and drug delivery. *Chemico-Biological Interactions* **2020**, *332*, 109305 ,https://doi.org/10.1016/j.cbi.2020.109305.

25. Cameron, L. P.; Tombari, R. J.; Lu, J.; Pell, A. J.; Hurley, Z. Q.; Ehinger, Y.; & Olson, D. E. A non-hallucinogenic psychedelic analogue with therapeutic potential. *Nature* **2021**, *589*, 474-479, https://doi.org/10.1038/s41586-020-3008-z.

26. Khwaza, V.; Oyedeji, O. O.; Aderibigbe, B. A. Anti-viral activities of oleanolic acid and its analogues. *Molecules* **2018**, *23*, 2300, https://doi.org/10.3390/molecules23092300.

27. Kumari, A.; Karnatak, M.; Singh, D.; Shankar, R.;Jat, J. L.; Sharma, S.;& Verma, V. P. Current scenario of artemisinin and its analogues for antimalarial activity. *European journal of medicinal chemistry* **2019,***163*, 804-829, https://doi.org/10.1016/j.ejmech.2018.12.007.

28. Manjunatha, B.; Bodke, Y. D.; Nagaraja, O.; Nagaraju, G.; Sridhar, M. A. Coumarin-Benzothiazole Based Azo Dyes: Synthesis, Characterization, Computational, Photophysical and Biological Studies. *Journal of Molecular Structure* **2021**, *1246*, 131170, https://doi.org/10.1016/j.molstruc.2021.131170.

29. Shin, H. K.; Lee, S.; Oh, H. N.; Yoo, D.; Park, S.; Kim, W. K.;& Kang, M. G. Development of blood brain barrier permeation prediction models for organic and inorganic biocidal active substances. *Chemosphere* **2021**, *277*,130330, https://doi.org/10.1016/j.chemosphere.2021.130330.

30. Abdul-Hammed, M.; Adedotun, I. O.; Olajide, M.; Irabor, C. O.; Afolabi, T. I.;Gbadebo, I. O.; &Ramasami, P. Virtual screening, ADMET profiling, PASS prediction, and bioactivity studies of potential inhibitory roles of alkaloids, phytosterols, and flavonoids against COVID-19 main protease (Mpro). *Natural product research* **2022**,*36*, 3110-3116, https://doi.org/10.1080/14786419.2021.1935933.

31. Bilgicli, H. G.; Ergon, D.; Taslimi, P.; Tüzün, B.; Kuru, İ. A.; Zengin, M.; Gülçin, İ. Novel propanolamine derivatives attached to 2-metoxifenol moiety: Synthesis, characterization, biological properties, and molecular docking studies. *Bioorganic Chemistry* **2020**, *101*, 103969, https://doi.org/10.1016/j.bioorg.2020.103969.

Supplementary materials

1. NMR and LC-MS data of new compounds
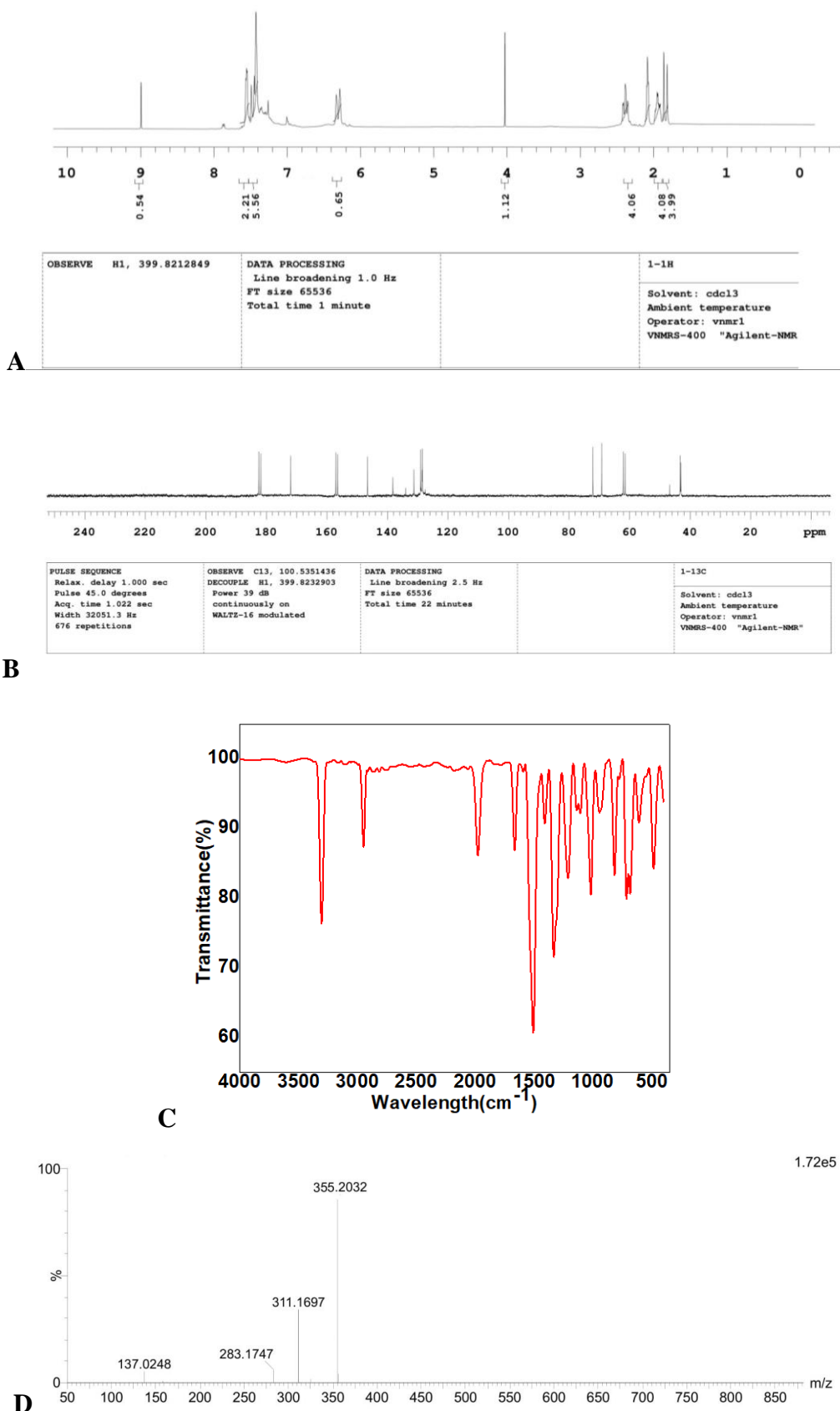
Figure S1. (Z)-4-(2-(((1H-pyrrol-2-yl)methylene)amino)ethyl)-N-phenylpipera zine-1-carbothioamide (5a).
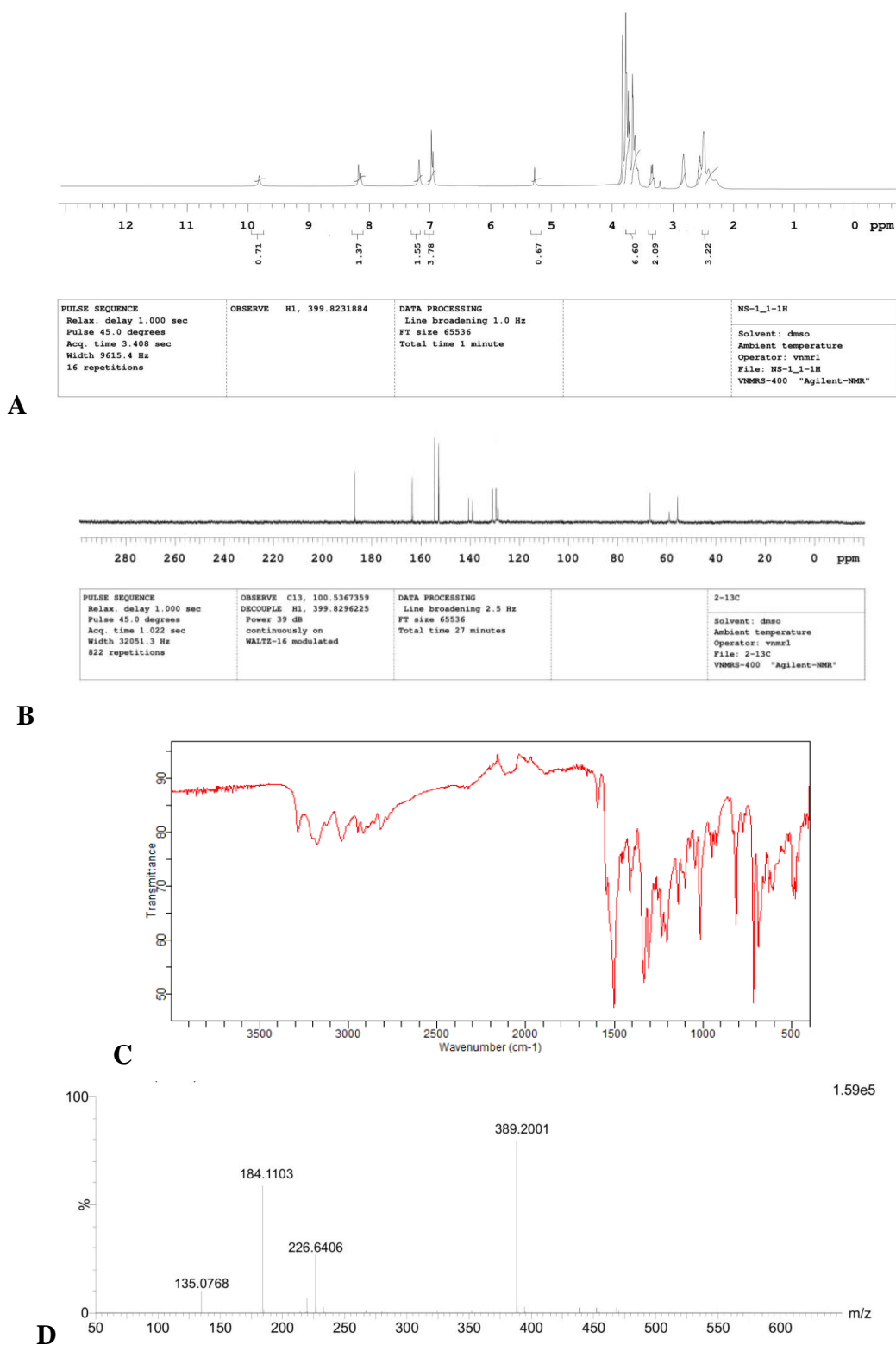[NOTE: A. 1H NMR spectra, B.13C NMR spectra, C. FTIR and D. LC-MS]
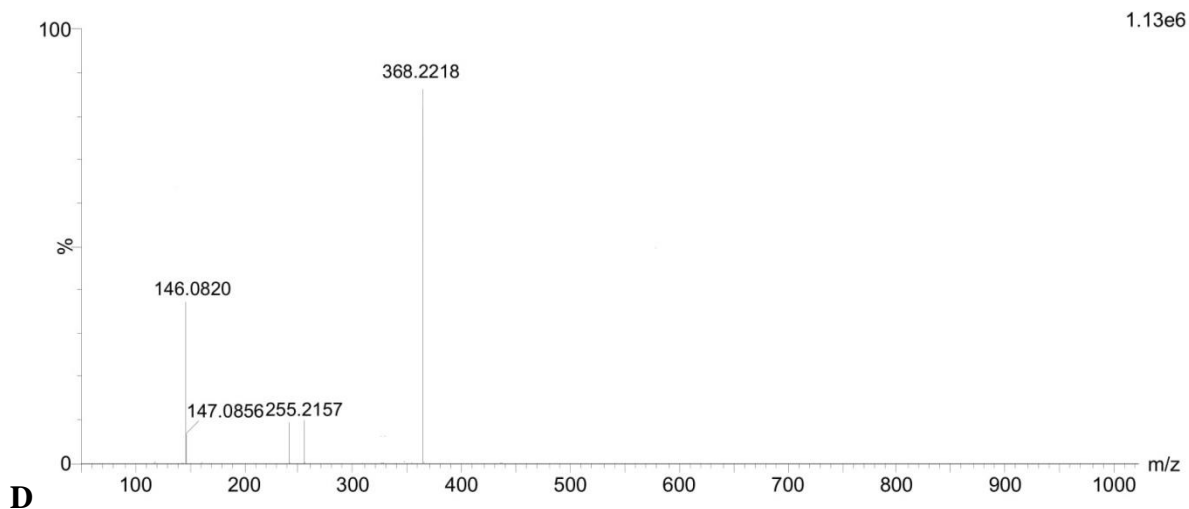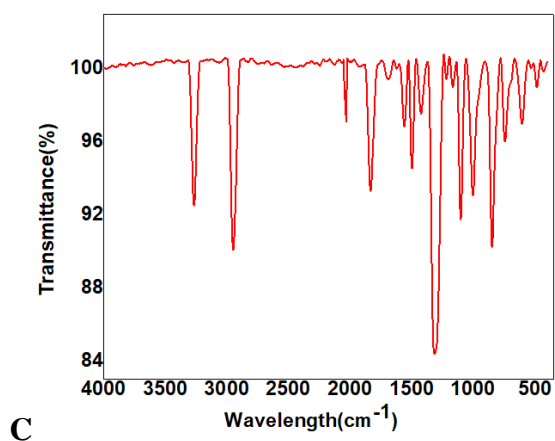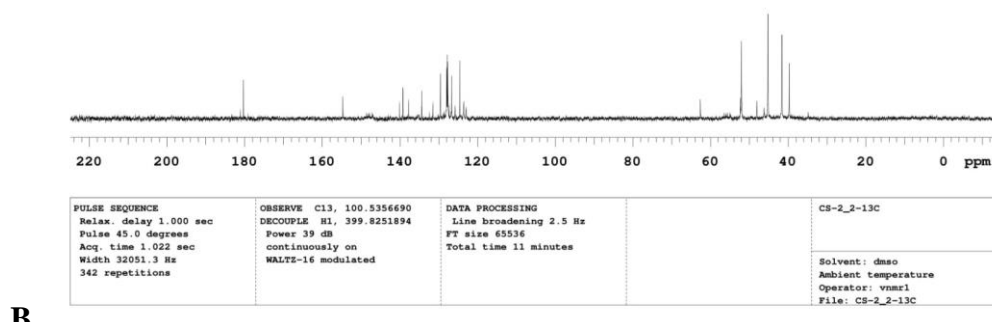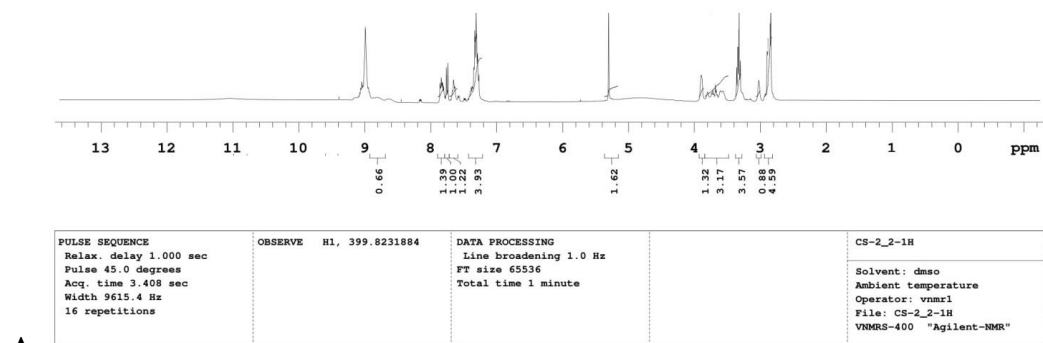
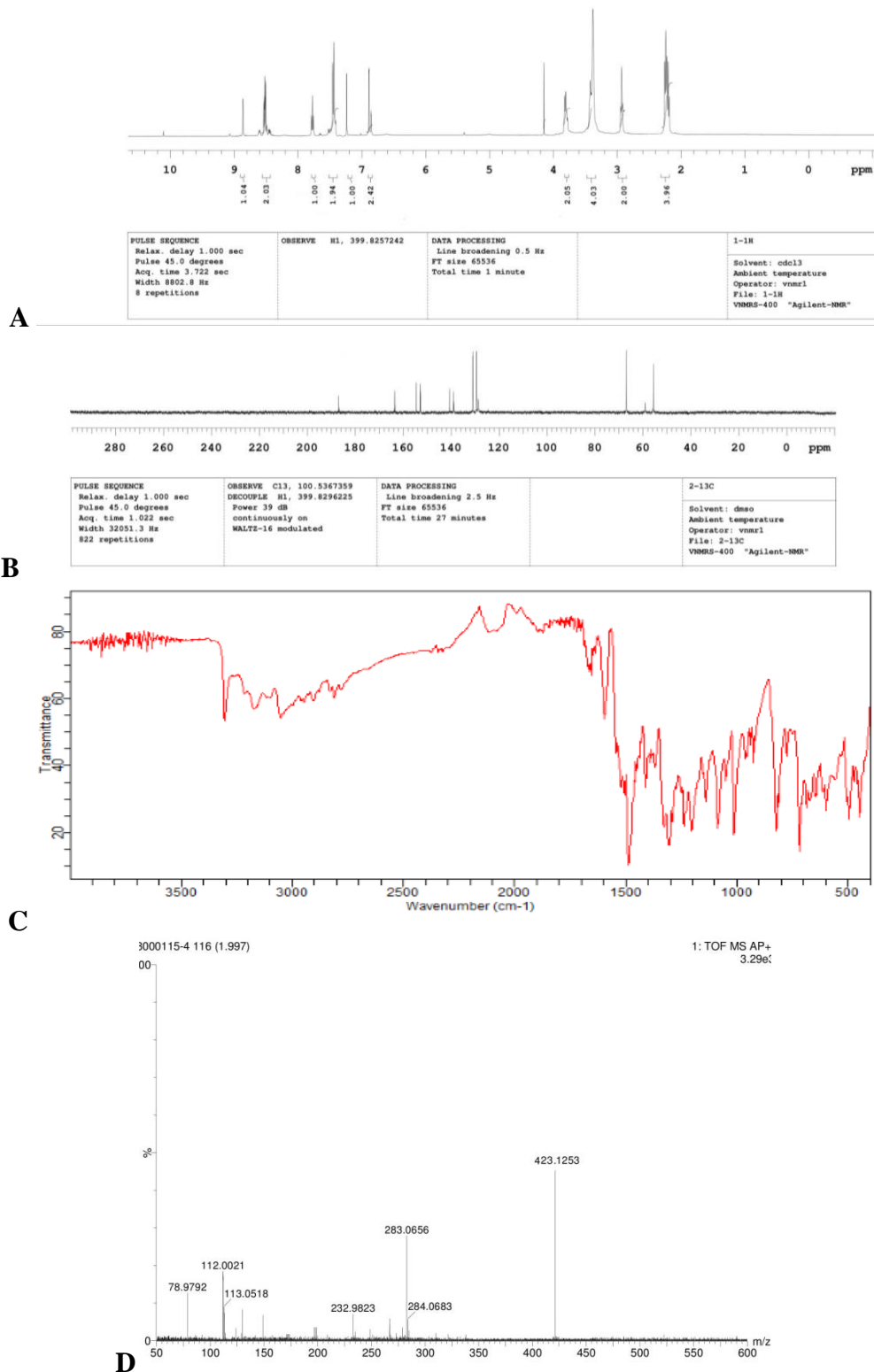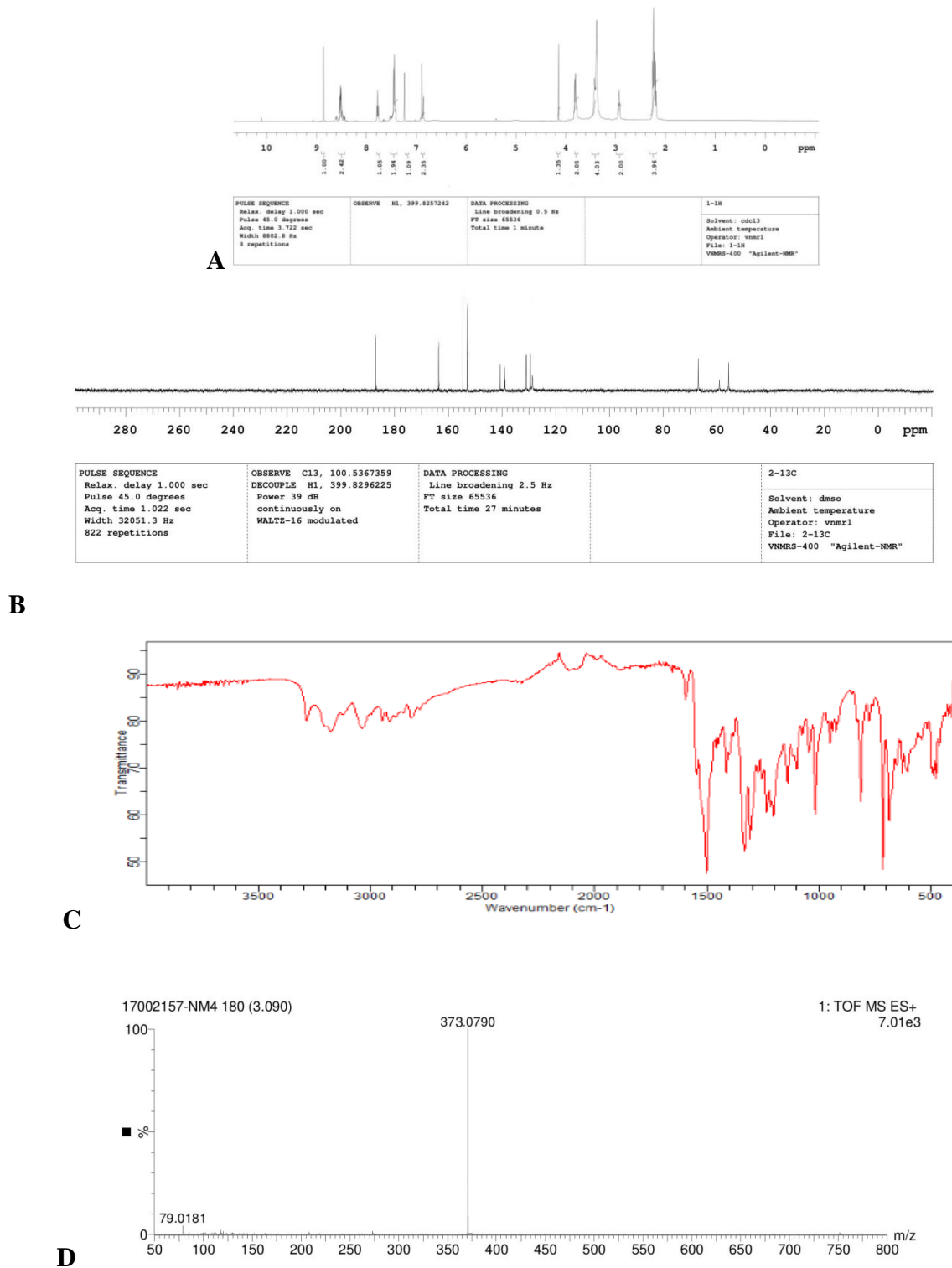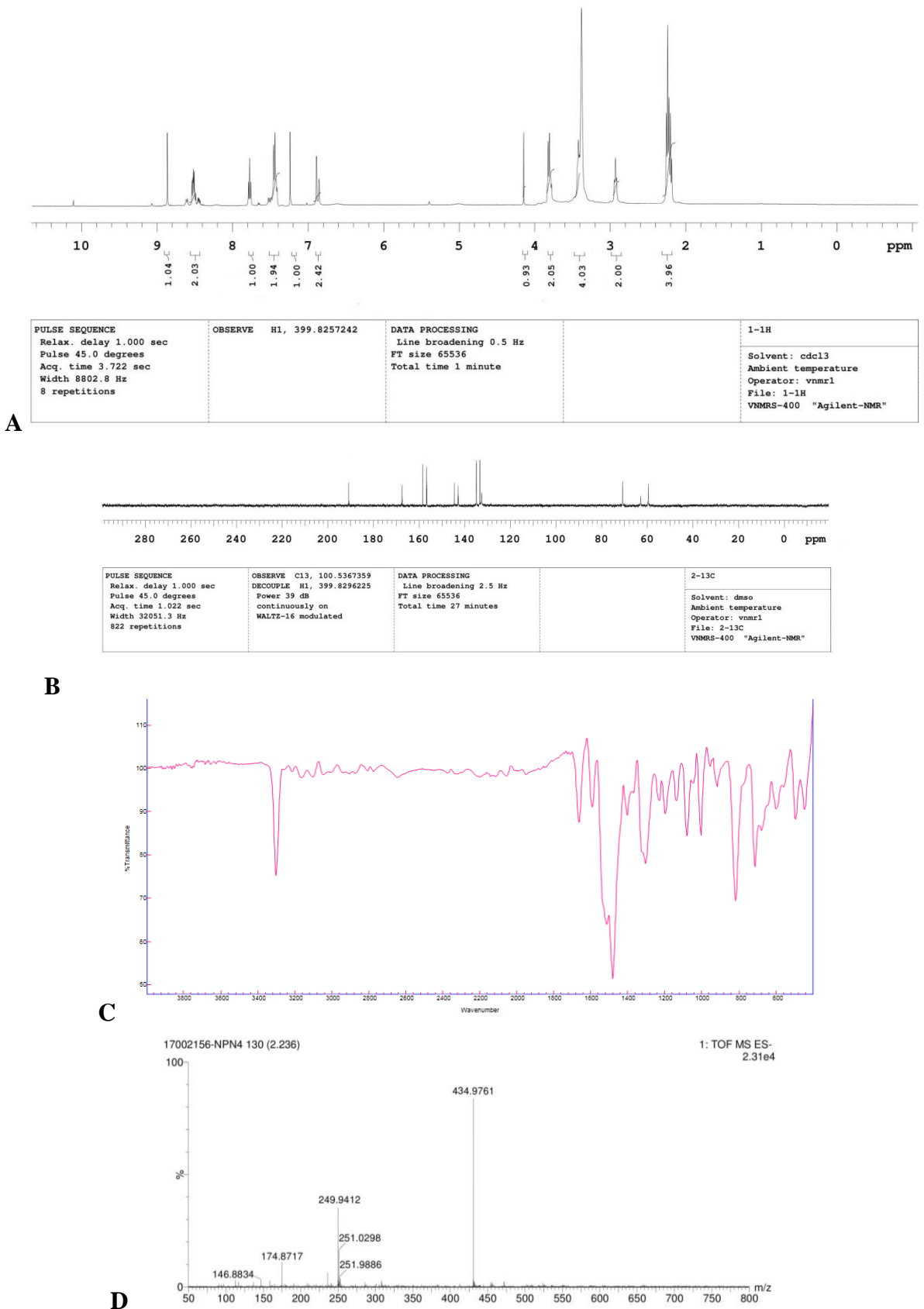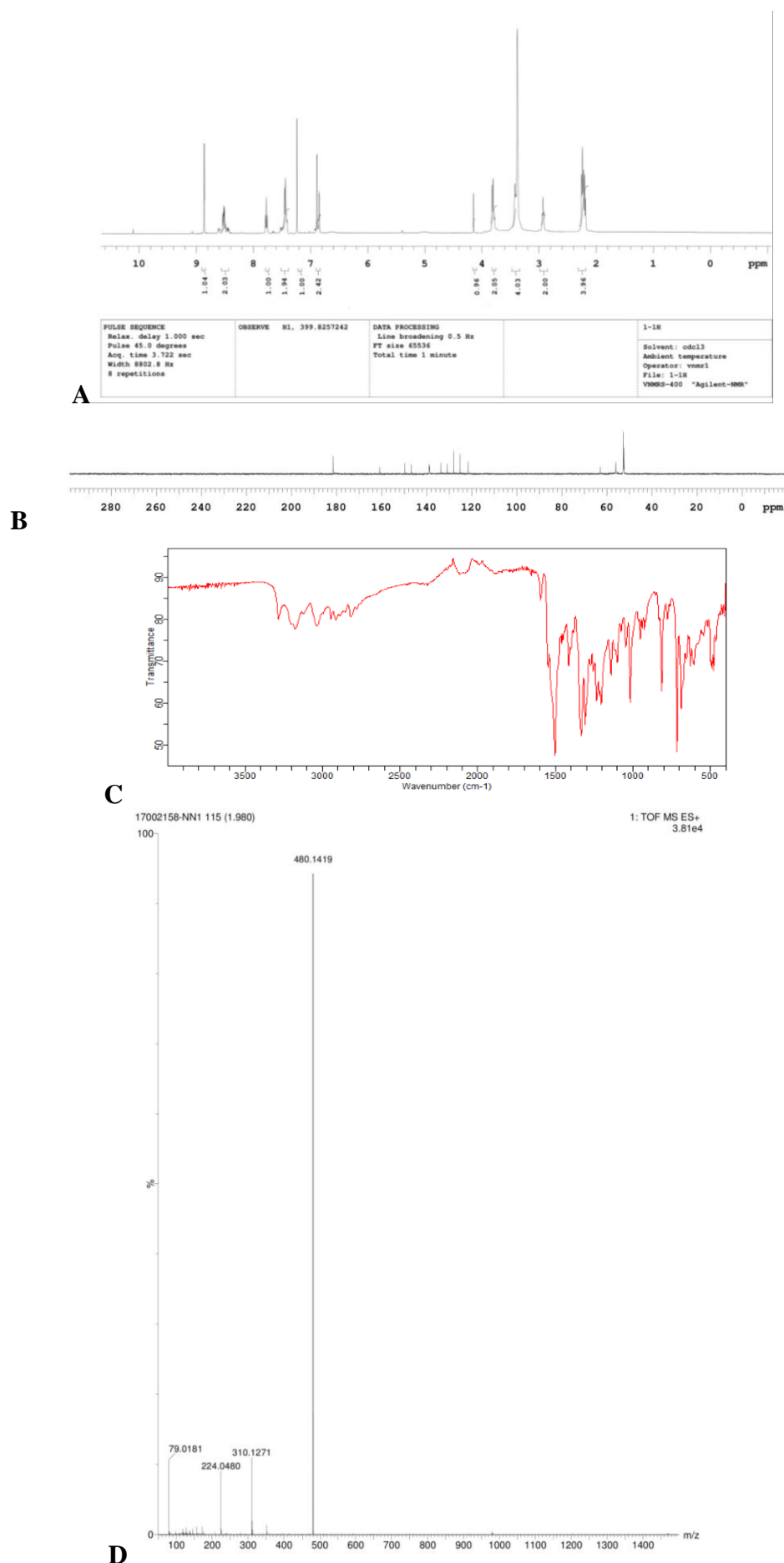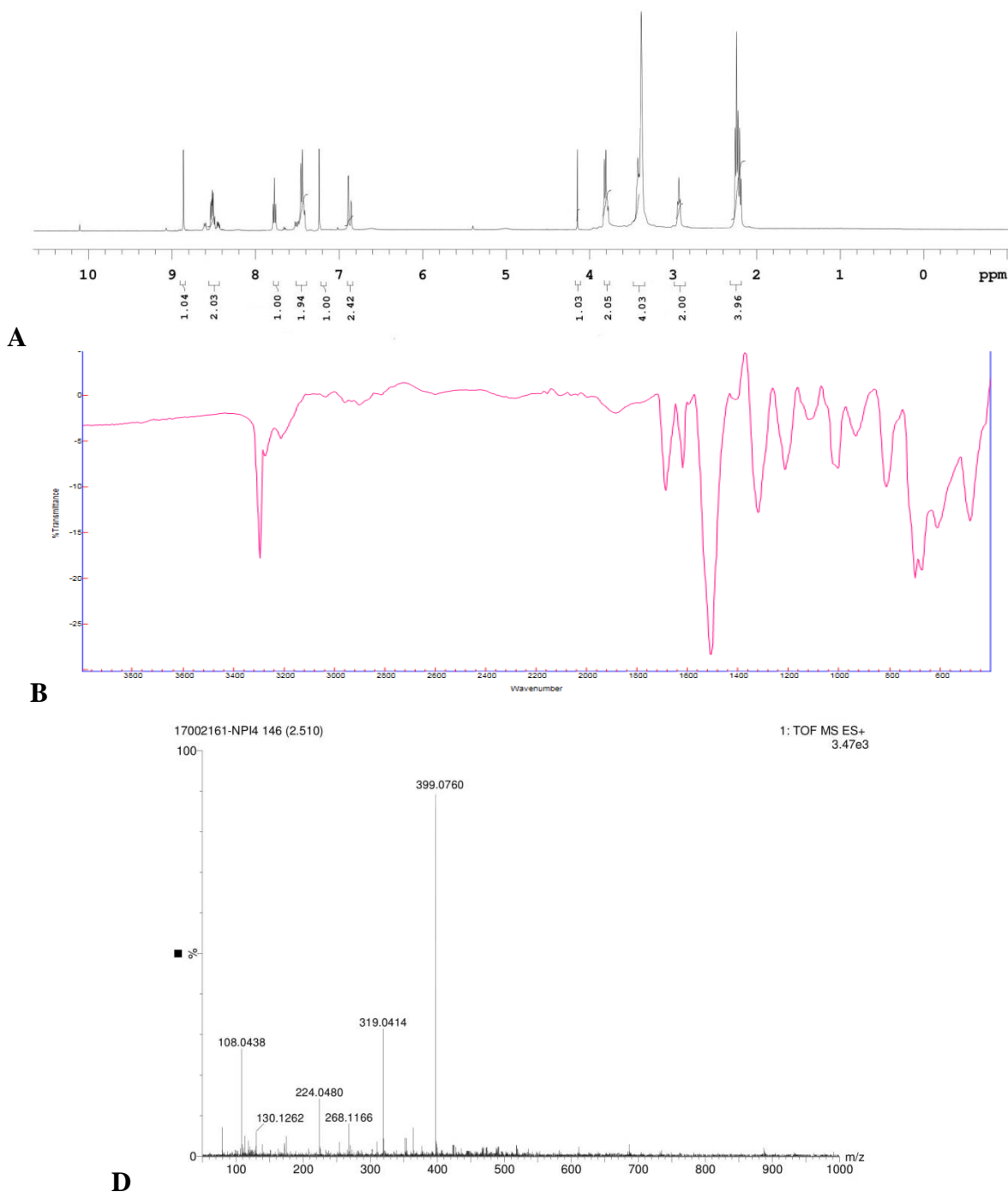**Figure S2.** (Z)-4-(2-(((1H-pyrrol-2-yl)methylene)amino)ethyl)-N-(p-tolyl)piperazi ne carbothioamide (5b).

Figure S3. (Z)-4-(2-(((1H-pyrrol-2-yl) methylene) amino) ethyl)-N-(4-methoxyphenyl) piperazine-1-carbothioamide (5c).
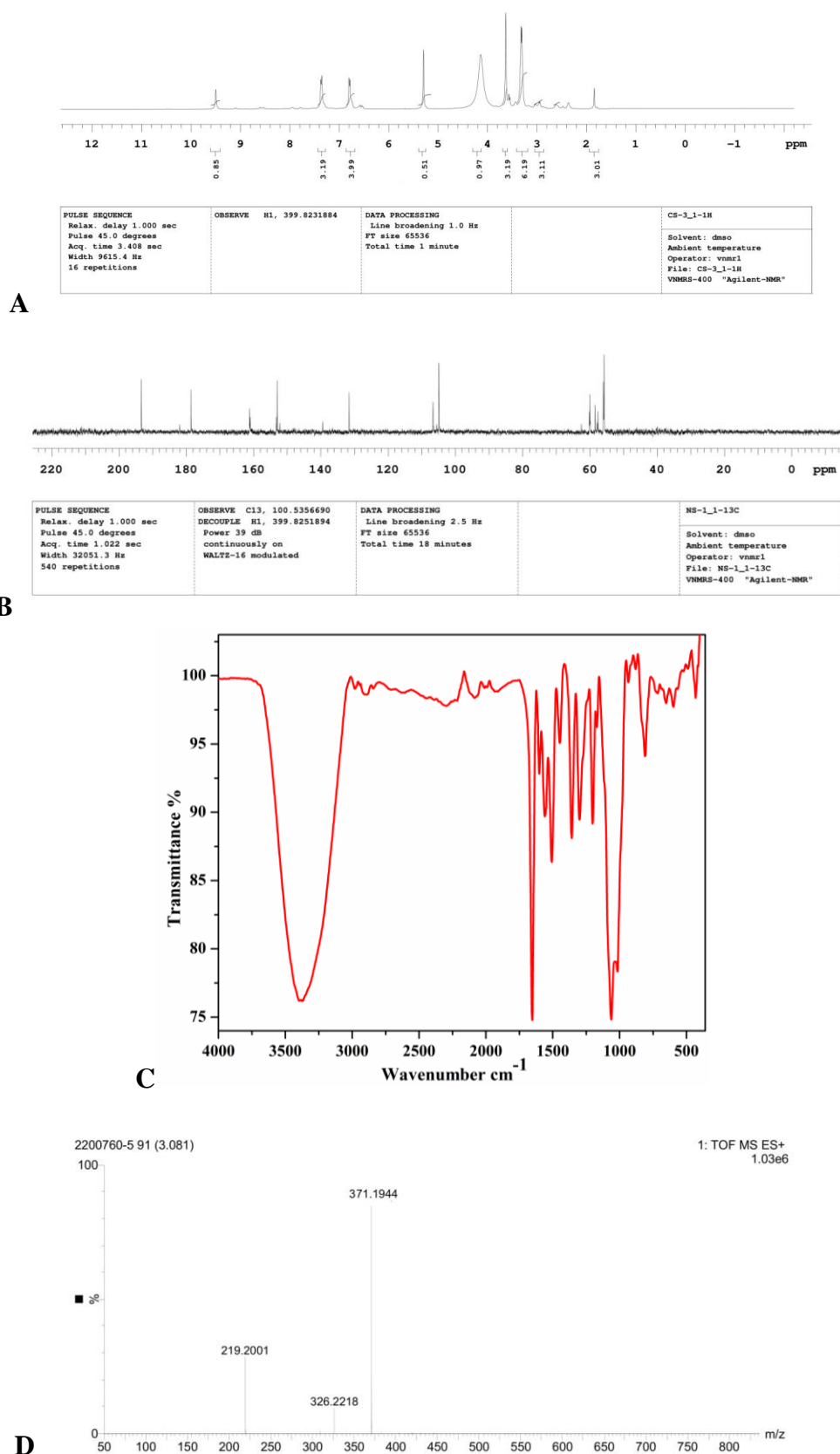
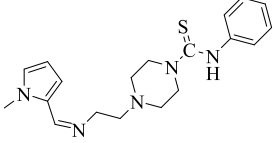**Figure S4.** (Z)-4-(2-(((1H-pyrrol-2-yl) methylene) amino) ethyl)-N-(4-hydroxyphenyl) piperazine-1-carbothioamide (5d).
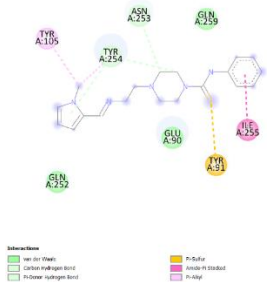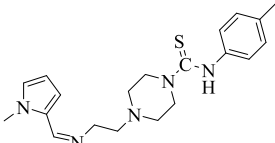
A

B

C

D

Figure S5. (Z)-4-(2-(((1H-pyrrol-2-yl) methylene) amino) ethyl)-N-(4-chlorophenyl) piperazine-1-carbothioamide (5e).

Figure S5. (Z)-4-(2-(((1H-pyrrol-2-yl) methylene) amino) ethyl)-N-(3,5-dichlorophenyl) piperazine-1-carbothioamide (5h).

Figure S6. (Z)-4-(2-(((1H-pyrrol-2-yl) methylene) amino) ethyl)-N-(4-fluorophenyl) piperazine-1-carbothioamide(5i).

Figure S7. (Z)-4-(2-(((1H-pyrrol-2-yl) methylene) amino) ethyl)-N-(4-bromophenyl) piperazine-1-carbothioamide (5j).

Figure S8. Z)-4-(2-(((1H-pyrrol-2-yl) methylene) amino) ethyl)-N-(4-iodophenyl) piperazine-1-carbothioamide (5k).

A

B

D
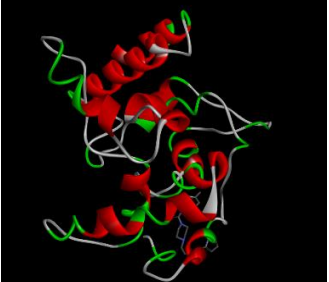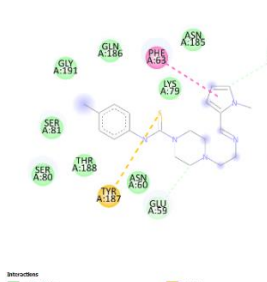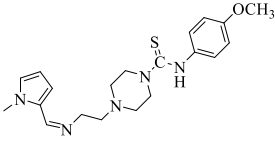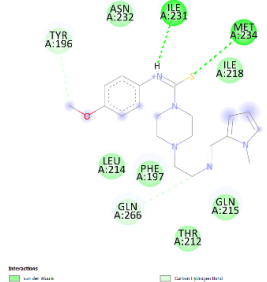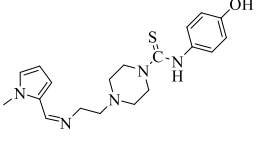
Figure S9. (Z)-4-(2-(((1H-pyrrol-2-yl) methylene) amino) ethyl)-N-(4-nitrophenyl) piperazine-1-carbothioamide (5l).

Table S1. Predicted biological activities of compounds 5(a-e), Pa (probability "to be active"), Pi (probability "to be inactive").

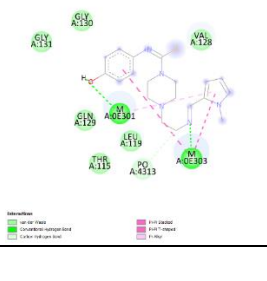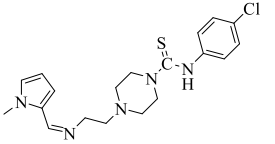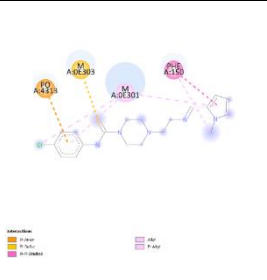| Activity	5a		5b		5c		5d		5e		5f	
	Pa	Pi	Pa	Pi	Pa	Pi	Pa	Pi	Pa	Pi	Pa	Pi
Chemo sensitizer	0.596	0.007	0.572	0.009	0.576	0.009	0.585	0.008	0.578	0.009	0.566	0.010
Histone deacetylase stimulant	0.500	0.003	0.409	0.003	0.426	0.003	0.465	0.003	0.372	0.003	0.332	0.004
Antineoplastic (pancreatic cancer)	0.299	0.059	0.285	0.070	0.286	0.070	0.285	0.070	0.277	0.078	0.285	0.071
Polarization stimulates	0.820	0.002	0.805	0.002	0.798	0.002	0.804	0.002	0.813	0.002	0.806	0.002
Antiprotozoal (Amoeba)	0.275	0.092	0.277	0.090	0.251	0.126	0.303	0.066	0.294	0.073	0.259	0.114
Protein kinase (ck1) epsilon inhibitor	0.188	0.037	0.170	0.055	0.101	0.097	0.173	0.052	0.187	0.037	0.202	0.028
Cytidine deaminase inhibitor	0.241	0.015	0.259	0.012	0.246	0.014	0.183	0.028	0.222	0.018	0.229	0.017
Antineoplastic (lung cancer)	0.163	0.090	0.155	0.096	0.195	0.072	0.166	0.088	0.137	0.114	0.133	0.118
Autotoxin inhibitor	0.217	0.002	0.203	0.003	0.201	0.003	0.203	0.003	0.205	0.003	0.203	0.003
Chemo sensitizer	0.606	0.006	0.578	0.009	0.560	0.011	0.801	0.002	0.608	0.002	0.822	0.002
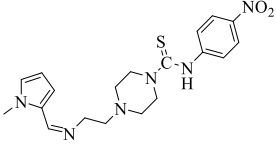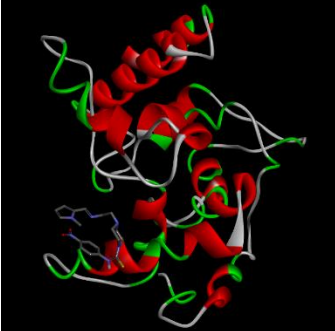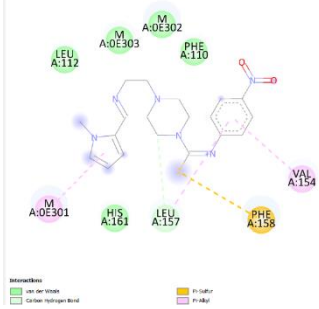
Activity	5a		5b		5c		5d		5e		5f	
	Pa	Pi	Pa	Pi	Pa	Pi	Pa	Pi	Pa	Pi	Pa	Pi
Histone deacetylase stimulant	0.333	0.003	0.341	0.003	0.387	0.003	0.366	0.003	0.336	0.003	0.453	0.003
Antineoplastic (pancreatic cancer)	0.253	0.102	0.282	0.073	0.282	0.073	0.340	0.036	0.363	0.027	0.349	0.032
Polarisation stimulant	0.804	0.002	0.809	0.002	0.804	0.002	0.801	0.002	0.801	0.002	0.822	0.002
Antiprotozoal (Amoeba)	0.239	0.149	0.278	0.088	0.241	0.144	0.308	0.063	0.294	0.073	0.408	0.024
Protein kinas(CK1) epsilon inhibitor	0.181	0.044	0.196	0.032	0.211	0.023	0.221	0.019	0.157	0.071	0.157	0.071
Cytidine deaminase inhibitor	0.245	0.014	0.195	0.025	0.192	0.026	0.288	0.009	0.125	0.057	0.299	0.008
Antineoplastic (lung cancer)	0.138	0.112	0.131	0.121	0.131	0.120	0.145	0.105	0.135	0.116	0.163	0.090
Autotoxin inhibitor	0.203	0.003	0.207	0.003	0.210	0.003	0.198	0.003	0.220	0.002	0.207	0.003

Table S2. Molecular docking interactive map of ligands **5(a-l)** and antibiotic streptomycin for **6FTB** of binding deep inside the active site, depicting the best docking pose showing 2D respectively.

Compound	Structure Protein Id: 6FTB	3D	2D	Binding energy
5a				-4.43
5b				-4.17
5c				-3.83
5d				-6.95
5e				-3.98

Compound	Structure Protein Id: 6FTB	3D	2D	Binding energy
5f				-4.19
5g				-4.20
5h				-4.23
5i				-3.48
5j				-4.32
5k				-5.17

Compound	Structure Protein Id: 6FTB	3D	2D	Binding energy
5l				-4.38

Table S3. Molecular docking scores of synthesized analogs and antibiotic streptomycin against 6FTB proteins.

Protein Id	Compound Name	Binding energy	Binding interaction
6FTB	5a	-4.43	GLN A:259,ASN A:256 – Van der Waals, GLU A90, GLU A:252 – Carbon hydrogen bond, TYR A:105 – pi alkyl, ILE A:255 – amide pi stackled, TYR A: 91 – pi sulfur.
	5b	-4.17	ASN A:185, GLN A:186, GLY A:191, LYS A:79, SER A:81, THR A:188, SER A:80,TYR A:62, ASN A:60 – Van der waals, ASN A:78, GLU A:59 – carbo hydrogen bond, PHE A:63 – Pi-Pi T shaped, TYR A:187 – Pi- Sulfur.
	5c	-3.83	ILE A:231, MET A:234 – conventional hydrogen bond, ILE A:218,ASN A:232,LEU A:214,PHE A:197,GLN A:215,THR A:212 – Van der waals, TYR A:196,GLN A:266 – carbon hydrogen bond.
	5d	-6.95	M A:0E301, M A:0E303 – conventional hydrogen bond, PO A:4313 – carbon hydrogen bond, GLY A:130,GLY A:131,GLN A:129 LEU A:119,THR A:115 – Van der waals.
	5e	-3.98	PO A: 4313 – pi anion, M A: 0E303 – pi sulfur, M A: OE301- pi alkyl, PHE A: 150 – pi-pi stackled.
	5f	-4.19	PO A: 4313 – conventional hydrogen bond, LEU A: 119, THR A: 115, M A: 0E303 – Van der waals, PHE A: 150 – pi-pi stackled, M A: 0E301 – pi- alkyl and alkyl, PO A: 4313 – pi-anion.
	5g	-4.20	M A:0E301, M A:0E303, M A:0E302, HIS A:161, LEU A:112 LYS A:155 – van der waals, PHE A:110, PHE A:158 – pi-pi stackled, LEU A:157, VAL A:154 – pi-alkyl and alkyl.
	5h	-4.23	LEU A: 119 – pi-sigma, M A: 0E301, M A: 0E303 – alkyl and pi-alkyl, PHE A: 150 – van der waals, PO A: 4313 – attractive charge.
	5i	-3.48	MET A:234, ILE A:231, ASN A:232 – conventional hydrogen bond, LEU A:214, , GLN A:215, THR A:212,LEU A:267,ILE A:218, PHE A:197- van der waals GLN A:266 - – carbon hydrogen bond.
	5j	-4.32	LYS A: 79 – pi-cation, SER A:81, TYR A: 62, SER A:80 – carbon hydrogen bond, PHE A:63,ASN A:78, ASN A:60, GLN A:186, TYR A:187, THR A:188 – van der waals, LYS A:75 – alkyl and pi-alkyl.
	5k	-5.17	M A: 0E303 – carbon hydrogen bond, PHE A:158, M A:0E303, HIS A:161 – van der waals, PHE A:110 – pi-pi stackled, VAL A:154, M A:0E301, LEU A:112, LEU A:157 – alkyl and pi-alkyl.
	5l	-4.38	PHE A: 158 – pi-sulfur, M A:0E301, VAL A:154 – pi-alkyl, LEU A:157 – carbon hydrogen bond, LEU A:112, HIS A:161, M A:0E303, M A:0E302, PHE A:110 – van der waals.
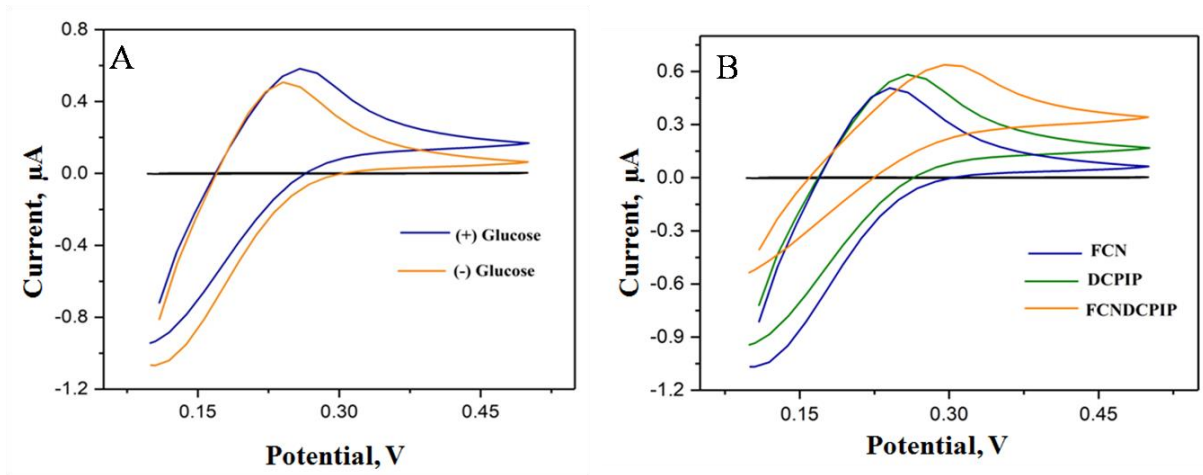
Figure S10. A) The cyclic voltammogram (CV) of glucose (+) and (-) for metabolic state of MRSA. **B)** The cyclic voltammogram (CV) of FCN (single mediator), DCPIP (single mediator) and FCN-DCPIP (double mediator) against MRSA.